Basin Research
EAGE
Basin Research (2017) 1–32, doi: 10.1111/bre.12260

Tectono-sedimentary evolution of the Plio-Pleistocene Corinth rift, Greece

Robert L. Gawthorpe,* Mike R. Leeder,† Haralambos Kranis,‡ Emmanuel Skourtsos,‡ Julian E. Andrews,† Gijs A. Henstra,* Greg H. Mack,§ Martin Muravchik,* Jenni A. Turner† and Michael Stamatakis‡

**Basin and Reservoir Studies Group, Department of Earth Science, University of Bergen, Bergen, Norway*
†School of Environmental Sciences, University of East Anglia, Norwich, UK
‡Department of Geology and Geoenviroment, National & Kapodistrian University of Athens, Athens, Greece
§Department of Geological Sciences, New Mexico State University, Las Cruces, NM, USA

ABSTRACT

The onshore central Corinth rift contains a syn-rift succession >3 km thick deposited in 5–15 km-wide tilt blocks, all now inactive, uplifted and deeply incised. This part of the rift records upward deepening from fluviatile to lake-margin conditions and finally to sub-lacustrine turbidite channel and lobe complexes, and deep-water lacustrine conditions (Lake Corinth) were established over most of the rift by 3.6 Ma. This succession represents the first of two phases of rift development – Rift 1 from 5.0–3.6 to 2.2–1.8 Ma and Rift 2 from 2.2–1.8 Ma to present. Rift 1 developed as a 30 km-wide zone of distributed normal faulting. The lake was fed by four major N- to NE-flowing antecedent drainages along the southern rift flank. These sourced an axial fluvial system, Gilbert fan deltas and deep lacustrine turbidite channel and lobe complexes. The onset of Rift 2 and abandonment of Rift 1 involved a 30 km northward shift in the locus of rifting. In the west, giant Gilbert deltas built into a deepening lake depocentre in the hanging wall of the newly developing southern border fault system. Footwall and regional uplift progressively destroyed Lake Corinth in the central and eastern parts of the rift, producing a staircase of deltaic and, following drainage reversal, shallow marine terraces descending from >1000 m to present-day sea level. The growth, linkage and death of normal faults during the two phases of rifting are interpreted to reflect self-organization and strain localization along co-linear border faults. In the west, interaction with the Patras rift occurred along the major Patras dextral strike-slip fault. This led to enhanced migration of fault activity, uplift and incision of some early Rift 2 fan deltas, and opening of the Rion Straits at *ca.* 400–600 ka. The landscape and stratigraphic evolution of the rift was strongly influenced by regional palaeotopographic variations and local antecedent drainage, both inherited from the Hellenide fold and thrust belt.

INTRODUCTION

Extension across the Gulf of Corinth (Fig. 1) is fast and young – it is one of the planet's most rapidly extending continental rifts – and geodetic extension rates reach 15 mm $year^{-1}$, with maximum Holocene rift flank uplift approaching 3 mm $year^{-1}$ (e.g. Davies *et al.*, 1997; Clarke *et al.*, 1998; Briole *et al.*, 2000; Avallone *et al.*, 2004; Pirazzoli *et al.*, 2004; Bernard *et al.*, 2006). The area has been the focus of much groundbreaking research on continental rifting, and significant developments have come from onshore and offshore mapping, and stratigraphic and sedimentological studies relevant to basin evolution (e.g. Ori, 1989; Collier, 1990; Bentham *et al.*, 1991; Gawthorpe *et al.*, 1994; Leeder *et al.*, 2002, 2012; Lykousis *et al.*, 2007; Rohais *et al.*, 2007a; Bell *et al.*, 2009; Taylor *et al.*, 2011; Ford *et al.*, 2013, 2016; Nixon *et al.*, 2016). These studies have shown that rift development began with early syn-rift continental sedimentation located in numerous half-graben depocentres. Subsequent strain localization and northward migration of active faulting initiated accelerated subsidence, evidenced by giant fan deltas that prograded into water 300–600 m deep. Offshore geophysical data has led to an overall integrated interpretation of seismic stratigraphy and basin structure, whereas onshore studies have focused on specific study areas in the west and eastern parts of the rift and have developed largely separate stratigraphic frameworks and tectono-sedimentary interpretations.

Correspondence: Robert L. Gawthorpe, Department of Earth Science, University of Bergen, Allegaten, 41, 5020 Bergen, Norway. E-mail: rob.gawthorpe@uib.no

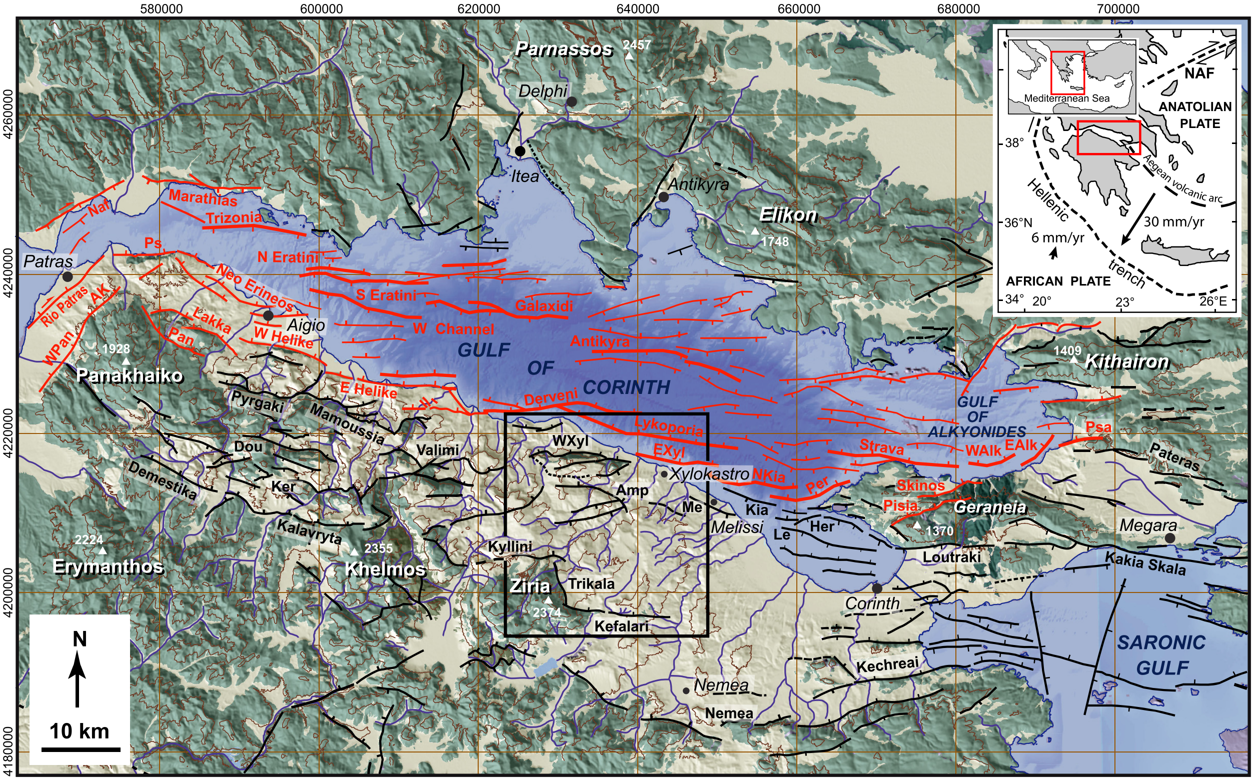

Fig. 1. General topography and geology of the Corinth rift. Pre-rift Hellenide basement (green), Plio-Pleistocene syn-rift sediments (tan) and main normal faults (faults active post 0.8 Ma – red; older, inactive faults – black). Contour interval = 500 m. Location of detailed central, onshore study area of Fig. 2 also shown. Note higher topographic relief north and south of the Gulf of Corinth towards the west. Inset shows study area in the context of Aegean/Mediterranean tectonic boundaries and plate motions. Offshore faults from Nixon *et al.* (2016); onshore faults from the authors' own mapping and Ford *et al.* (2013, 2016); Rohais *et al.* (2007a). Fault names in bold; abbreviations – AK, Ano Kastritsi fault; Amp, Amphithea fault; Dou, Doumena fault; EAlk, East Alkyonides fault; EXyl, East Xylokastro fault; Her, Heraion fault; Ker, Kerpini fault; Kia, Kiato fault; Le, Lechion fault; Me, Melissi fault; Naf, Nafpaktos fault; NKia, North Kiato fault; Pan, Panachaikon fault; Per, Perachora fault; Ps, Psathopyrgos fault; Psa, Psatha fault; WAlk, West Alkyonides fault; WPan, West Panachaikon fault; WXyl, West Xylokastro fault.

This paper presents new field observations of stratigraphy, sedimentology and structure from the relatively understudied central onshore Corinth rift. We use these, together with chronological control provided by dated volcanic ash (Leeder *et al.*, 2012), to: (a) integrate onshore studies within a new chronostratigraphic framework, and (b) combine this onshore work with recent offshore studies (e.g. Bell *et al.*, 2009; Taylor *et al.*, 2011; Nixon *et al.*, 2016) to present, for the first time, a coherent tectono-sedimentary analysis for the rift as a whole. We then discuss the implications of this work for rift basins globally.

GEOLOGICAL SETTING

The Corinth rift strikes E-W (Fig. 1) and is the most active of a series of late Tertiary rift basins developed within a diffuse zone of N-S extension of the former Hellenic orogen, between the North Anatolian fault and the Kephalonia fault/Hellenic subduction zone. The onset of rifting is partly constrained by radiometric dating of lavas and ash in eastern onshore outcrops (Collier & Dart, 1991; Leeder *et al.*, 2008) to early Pliocene or latest Miocene, *ca.* 5 Ma.

Geodetically measured N-S extension across the rift over the last 20 years increases from <5 mm year^{-1} in the east to 10–15 mm year^{-1} in the west (e.g. Clarke *et al.*, 1997; Davies *et al.*, 1997; Briole *et al.*, 2000; McClusky *et al.*, 2000; Avallone *et al.*, 2004; Bernard *et al.*, 2006; Floyd *et al.*, 2010). However, longer term stratigraphic estimates suggest greatest extension in the central part of the rift (Bell *et al.*, 2011; Nixon *et al.*, 2016). Ford *et al.* (2013) postulate that extension rates increased over time, from <1 mm year^{-1} in the late Pliocene/early Pleistocene to 3.4–4.8 mm year^{-1} in the mid-late Pleistocene, though these estimates lack direct chronology.

Active extension is localized on a network of mainly E-W-striking, N-dipping normal faults along the southern shores and into the offshore Gulf of Corinth (Fig. 1). These faults are up to 20 km long, with throws of up to several kilometres and dominantly dip-slip displacement, and are well-exposed where resistant pre-rift Mesozoic limestones and cherts are exposed in their footwalls. Major, but inactive, N- and S-dipping normal faults are imaged offshore and more continuously in a broad area of the north Peloponnesus, extending up to 30–40 km south of the Gulf of Corinth shoreline and around the Megara basin (Fig. 1).

Erosion of the Hellenide fold and thrust belt has been the main clastic sediment source to the entire rift (Skourtsos & Kranis, 2009; Ford *et al.*, 2013, 2016). Onshore tectono-sedimentary studies of Plio-Pleistocene syn-rift sediments have focused around the Megara basin, Perachora Peninsula and Corinth basin in the eastern part of the rift (e.g. Jackson *et al.*, 1982; Collier, 1990; Bentham *et al.*, 1991; Collier & Dart, 1991; Gawthorpe *et al.*, 1994; Mack *et al.*, 2006; Leeder *et al.*, 2008), and from Aigion to Derveni in the western part (e.g. Ori, 1989; Dart *et al.*, 1994; Gawthorpe *et al.*, 1994; Rohais *et al.*, 2007a,b; Ford *et al.*, 2013, 2016) (Fig. 1). Offshore in the Gulf of Corinth syn-rift sediments comprise an upper seismic unit (Nixon *et al.*, 2016), with alternating high-amplitude reflective and non-reflective seismic packages. Calibration of the youngest of these with shallow cores (Moretti *et al.*, 2004) suggests that they represent alternating marine and non-marine sedimentation related to 100 kyr glacio-eustatic cycles. An older seismic unit is separated from these sediments by a regional unconformity with an estimated age of 620 ka (Nixon *et al.*, 2016). A 1.5–2 Ma age for the base of the older seismic unit is estimated from thickness and decompacted sedimentation rates.

Our knowledge of the central onshore part of the rift is more limited. Following early reconnaissance studies (Keraudren & Sorel, 1987; Koutsouveli *et al.*, 1989; Doutsos & Piper, 1990; Seger & Alexander, 1993), recent discovery and precise radiometric dating of a calc-alkaline Stamatakis volcanic ash (Leeder *et al.*, 2012) highlights the potential of this part of the rift for developing a better chronostratigraphic understanding of the entire rift fill and its structural evolution. Our research focuses on the West Xylokastro fault, the Xylokastro fault block, the Xylokastro horst and the Amphithea fault block, which together dominate the northern part of the study area (Figs 1 and 2). South of the Amphithea fault, the Amphithea horst and Amphithea fault block are the main structural elements (Figs 1 and 2). The rift is bounded to the south by the interlinked Kyllini, Trikala and Kefalari faults, which separate the rift from northern Peloponnesus Hellenic basement (Figs 1 and 2).

STRATIGRAPHY AND SEDIMENTOLOGY

The Plio-Pleistocene syn-rift stratigraphic succession unconformably overlies pre-rift Mesozoic limestones and cherts of the Hellenide Pindos unit, with deeper units of the Hellenide thrust belt, including the Phyllites-Quartzites unit containing mica schists, quartzites and some metabasalts, locally exposed in the footwall to the southern rift border fault. We recognize four major syn-rift lithostratigraphic units, which have coherent assemblages of facies bounded by unconformities, major changes in facies, or faults. In stratigraphic order they are the Korfiotissa, Ano Pitsa, Pellini and Rethi-Dendro formations, and they record the progressive development of a late Pliocene to early Pleistocene lake depocentre, here termed Lake Corinth (Figs 2 and 3). They are partly time-equivalent to coarse-grained deltas in the west and south of the study area and may be unconformably overlain by Late Pleistocene shallow marine and delta deposits (Fig. 2). These stratigraphic units have been mapped over the study area at 1 : 25 000 scale and tied to previous studies to the west (Fig. 2). The formations are readily distinguished over most of the study area, but identification is more problematic in areas with landslides and heavy vegetation cover that lack extensive exposures (e.g. the south and west flanks of the Xylokastro and Amphithea horsts).

Korfiotissa Formation

The Korfiotissa Formation comprises 300–400 m of reddish-brown conglomerates, sandstones and siltstones named after the most extensive and well-exposed outcrops in the vicinity of Korfiotissa village on the southern Xylokastro horst. Here, it rests unconformably upon basement Pindos limestone, the contact displaying significant pre-rift basement topography (Figs 3a and 4a). To the south it is in faulted contact with marls and sandstones of the Rethi-Dendro Formation. Along the northern margin of the Xylokastro horst, the formation outcrops in rider blocks bounded by splays to the West Xylokastro fault (Fig. 2). A third area of outcrop, extensive but generally more poorly exposed, occurs on the Amphithea horst (Fig. 2). Here, the formation lies unconformably upon Pindos limestone in the footwall to the Amphithea fault; it has a faulted contact to the north with Rethi-Dendro Formation marls and a stratigraphic contact to the south with Ano Pitsa Formation marls and sandstones (Fig. 2).

We recognize two facies associations within the Korfiotissa Formation: (a) channelized conglomerates, and (b) intercalated sandstones and mudstones.

Channelized conglomerates

This facies association comprises storeys of thickly bedded, often channelized conglomerates up to 20 m thick

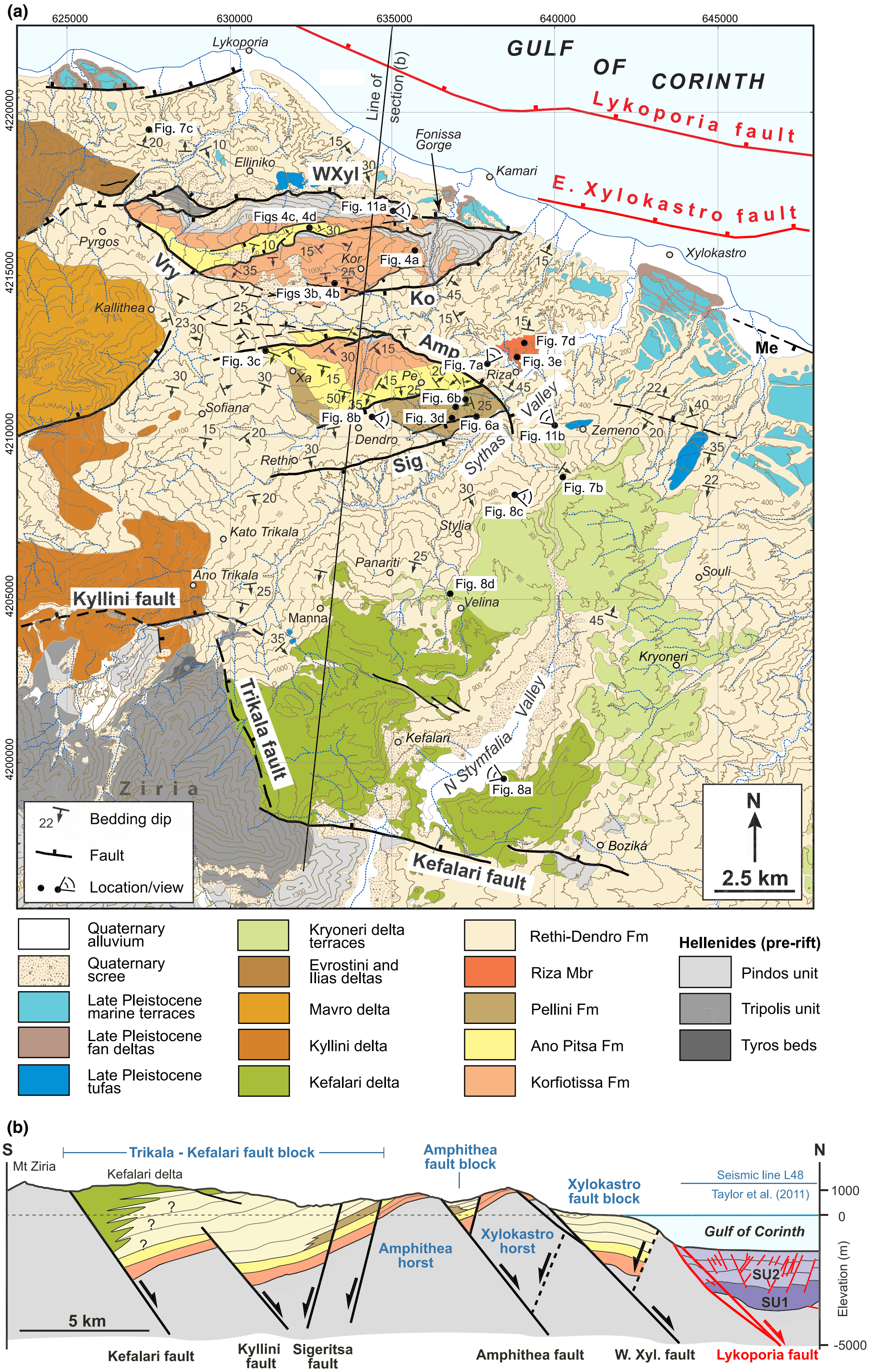
(a)
625000
630000
635000
640000
645000
4220000
4215000
4210000
4205000
4200000
GULF OF CORINTH
Lykoporia fault
E. Xylokastro fault
Line of section (b)
Lykoporia
Fonissa Gorge
Kamari
Xylokastro
Elliniko
WXyl
Pyrgos
Vry
Ko
Kor
Kallithea
Amp
Me
Xa
Pe
Riza
Sofiana
Dendro
Rethio
Sig
Sythas
Valley
Zemeno
Kato Trikala
Stylia
Panariti
Ano Trikala
Kyllini fault
Manna
Velina
Souli
Kryoneri
Trikala fault
Kefalari
N Stymfalia
Valley
Ziria
Kefalari fault
Boziká
Fig. 7c
Fig. 11a
Figs 4c, 4d
Fig. 4a
Figs 3b, 4b
Fig. 7d
Fig. 7a
Fig. 3e
Fig. 3c
Fig. 6b
Fig. 8b
Fig. 3d
Fig. 6a
Fig. 11b
Fig. 7b
Fig. 8c
Fig. 8d
Fig. 8a
Bedding dip
Fault
Location/view
N
2.5 km
Quaternary alluvium
Quaternary scree
Late Pleistocene marine terraces
Late Pleistocene fan deltas
Late Pleistocene tufas
Kryoneri delta terraces
Evrostini and Ilias deltas
Mavro delta
Kyllini delta
Kefalari delta
Rethi-Dendro Fm
Riza Mbr
Pellini Fm
Ano Pitsa Fm
Korfiotissa Fm
Hellenides (pre-rift)
Pindos unit
Tripolis unit
Tyros beds
(b)
S
N
Trikala - Kefalari fault block
Amphithea fault block
Xylokastro fault block
Mt Ziria
Kefalari delta
Seismic line L48
Taylor et al. (2011)
Gulf of Corinth
Amphithea horst
Xylokastro horst
SU2
SU1
1000
0
-5000
Elevation (m)
5 km
Kefalari fault
Kyllini fault
Sigeritsa fault
Amphithea fault
W. Xyl. fault
Lykoporia fault

Fig. 2. Detailed geology of the central onshore Corinth rift as mapped by the authors. (a) Geological map. (b) Representative cross-section including offshore geology from Taylor *et al.* (2011) with offshore seismic units (SU) 1 and 2 after Nixon *et al.* (2016). Faults active post 0.8 Ma – red; older, inactive faults – black. Fault abbreviations: Amp, Amphithea fault; Ko, Koutsa fault; Me, Melissi fault; Sig, Sigeritsa fault; Vry, Vryssoules fault; WXyl, West Xylokastro fault). Town abbreviations in italics: *Kor*, Korfiotissa; *Pe*, Pellini; *Xa*, Xanthochori.

(Figs 3b and 4b) and several tens of metres wide. The generally clast-supported and structureless conglomerate storeys rest abruptly on the underlying finer and thinner bedded units, and an imbricate fabric and rare cross-stratification are locally visible. The pebble- to cobble-grade clasts are usually sub- to well-rounded and comprise red and black chert, porcellanous and (rarer) oolitic limestone, and indurated light-brown sandstone. Metamorphic clasts are absent. Well-exposed roadcuts exhibit common lateral tonguing-out and bed sets of cross-stratification. Palaeocurrents are generally towards the east (Fig. 5), sub-parallel to fault strike.

Intercalated sandstones and mudstones

The second facies association is made up of thinner, irregular intercalations of structureless and cross-stratified coarse sandstones and silty mudstones, the latter with interbedded mottled reddish palaeosol horizons (Figs 3b and 4b). Need an extra line at the end of this paragraph to separate the description of the facies association from the overall interpretation of the formation, i.e. like the space between the 3rd order headings.

We deduce that the depositional environment was broadly continental and fluviatile, similar to that of early syn-rift deposits further west in the Corinth rift such as the Lithopetra and Ladopotamous formations (Rohais *et al.*, 2007a; Ford *et al.*, 2016; Hemelsdaël *et al.*, 2017). The well-rounded nature of the sedimentary clasts indicates a considerable transport distance, and clast types suggest an ultimate source dominated by Pindos limestone and flysch, probably also with recycling of older fluviatile clasts. The thicker conglomerate storeys represent the deposits of vigorous channels, the deeper erosive examples perhaps indicating episodes of channel incision (Bridge, 2003). Sandstone unit bar-forms are similar to modern examples from sandy braided rivers (Bridge, 1993; Lunt *et al.*, 2004), whilst the fine-grained facies are indicative of periodically ponded alluvial floodplains that received occasional floodwater incursions.

Ano Pitsa Formation

The Ano Pitsa Formation is 200–300 m thick and is mapped conformably overlying the Korfiotissa Formation on the Xylokastro and Amphithea horsts (Fig. 2), although the actual contacts are not exposed. The formation is highly variable in its lithofacies, which we group into four end-member facies associations: (a) calcareous mudstones and limestones, (b) mudstones and lignites, (c) channelised conglomerates, and d) well-sorted sandstones and conglomerates.

Calcareous mudstones and limestones

This predominantly fine-grained facies association is dominated by calcareous mudstones inter-bedded with 20–30 cm-thick, nodular micritic limestones and thicker (0.6–1.0 m) limestone beds with fine to granular calcareous sandstones (Fig. 3c). The mudstones mainly have variegated green-grey colours, sometimes tinged with purple mottles, and less common reddened horizons. Around Xanthochori the mudstones display incipient vertic soil fabrics and centimetre-sized calcareous nodules (Fig. 3c). The limestones contain coated grains, oncoids, possible charophyte stems and abundant reworked clasts and blocks (up to cobble size) of tufa stromatolites, some with exceptionally well-preserved radiating fibrous laminae (Fig. 4c, d). In a few places in situ tufa stromatolites up to 10 cm thick are present, some inter-constructed with chironimid larval tubes. Macrofossils are restricted to rare thin-shelled gastropods.

Mudstones and lignites

This facies association is also dominated by mudstone, but with much darker grey horizons passing into 8–15 cm-thick lignite seams. Some of the mudstones contain wood fragments and twigs coated with tufa. The lignite seams may be underlain by siltstones up to 60 cm thick with rootlets preserved in the upper parts. Nodular marlstones with thin-shelled gastropods including *Theodoxus* and other neritids, bithnyids and viviparids also occur, as well as thin, sharp-based calcite-cemented sandstones.

Channelized conglomerates

The third facies association comprises sharp-based and channelized conglomerates up to 20 m thick, with thinner, metre-scale sandstone beds (Fig. 3c). Clast type and provenance are identical to those of the Korfiotissa Formation, i.e. the Pindos unit. In exposures around the town of Pellini, at least four cycles, each around 5 m thick, comprise such conglomerates alternating with the mudstone/lignite association.

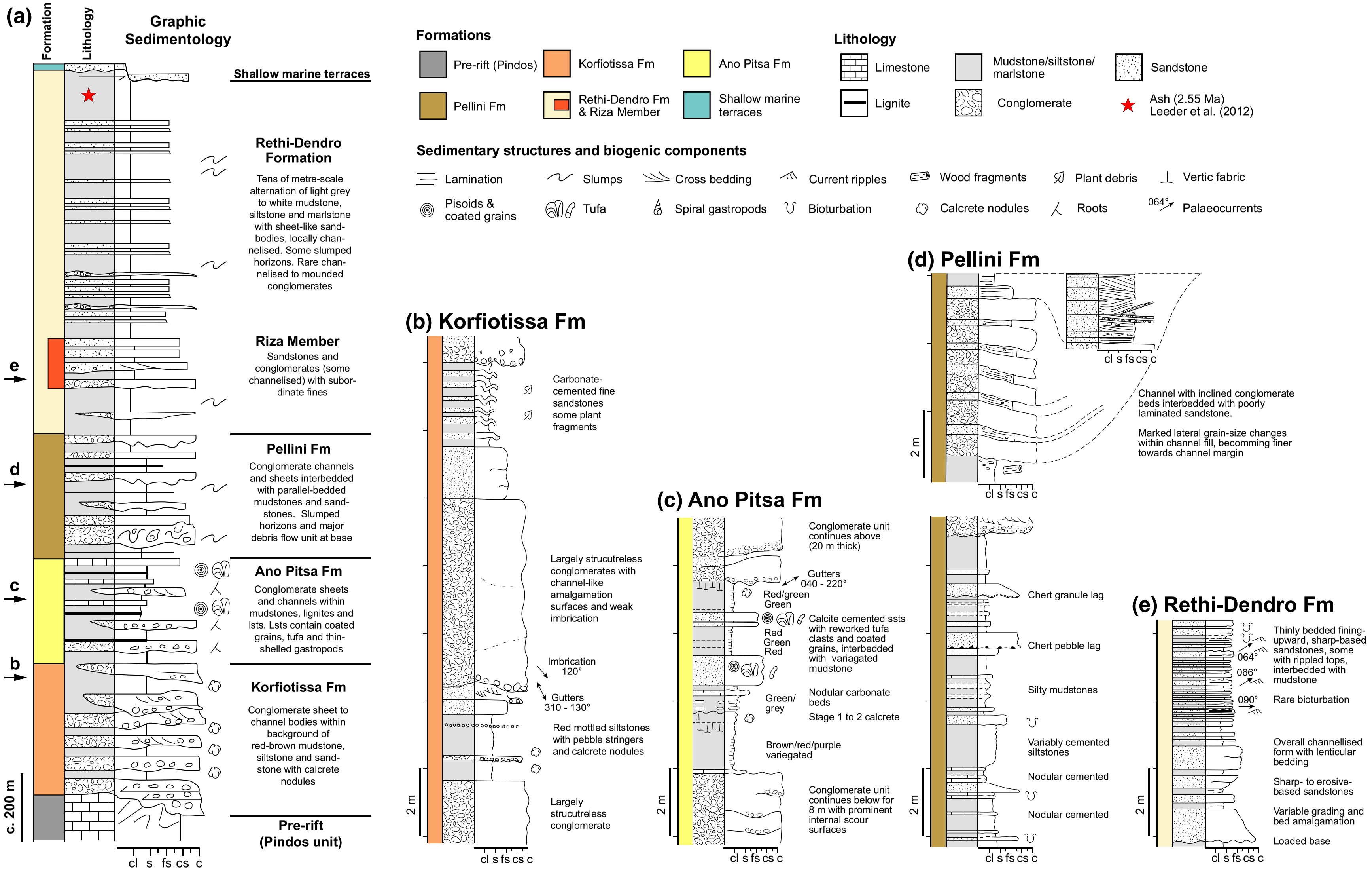

Fig. 3. Stratigraphy and sedimentological graphic logs. See text for full discussion. (a) Composite stratigraphic column for the Plio-Pleistocene succession illustrating the main formations. Arrows indicate approximate location of the representative sedimentary logs (b–e) that illustrate the main sedimentary features of the mapped formations (see Fig. 2 for location). (b) Korfiotissa Formation (UTM 0633503 4214660). (c) Ano Pitsa Formation (0631754 4212741). (d) Pellini Formation, parallel bedded mudstone, siltstone and sandstone (lower log; 0636973 4210634) and channelized conglomerates and sandstones (upper log; 0637075 4210858). (e) Rethi-Dendro Formation transition between sandstone-dominated facies association (lower part of log) and fines-dominated facies association (upper part of log) (0638878 4212408).

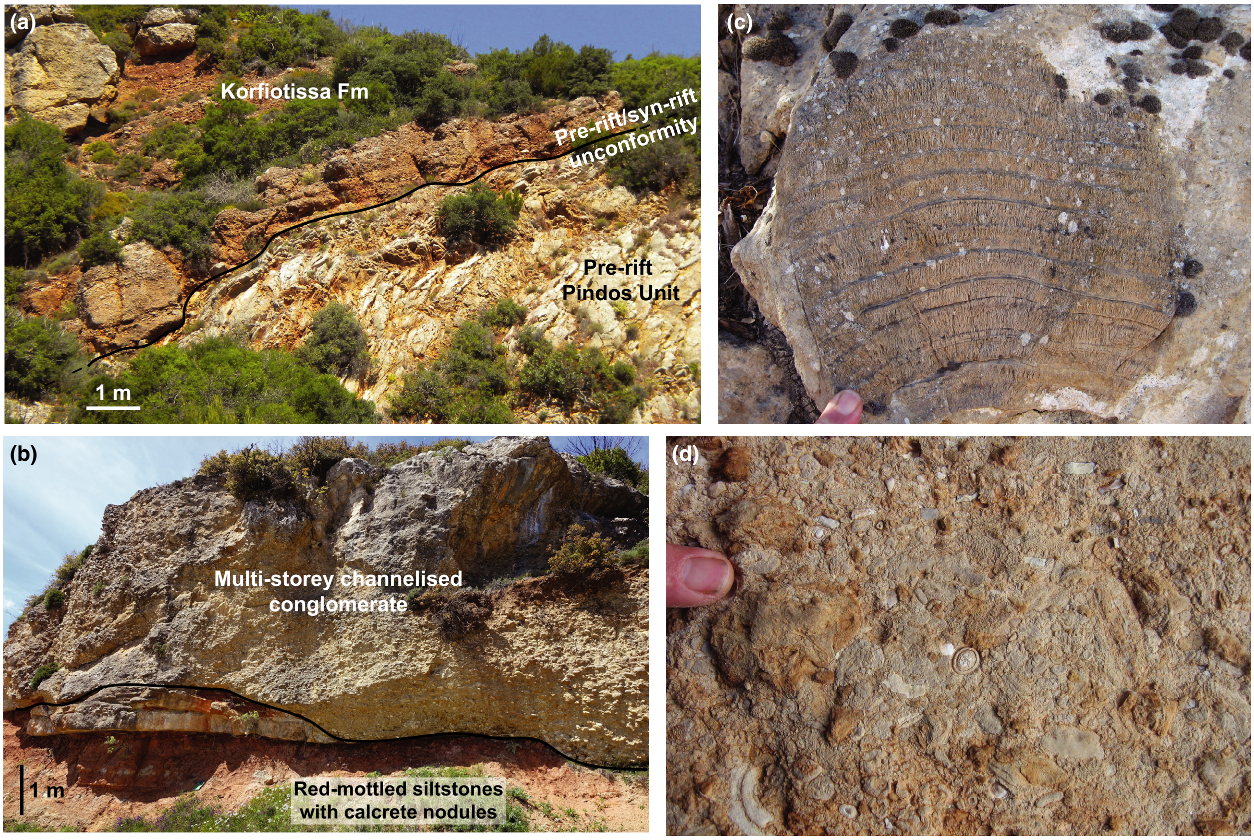

Fig. 4. Sedimentary characteristics of the Korfiotissa and Ano Pitsa formations (see Fig. 2 for location). (a) Basal unconformity with onlapping conglomerates of the Korfiotissa Formation, west flank of the Fonissa gorge, Xylokastro horst (0635778 4215838). (b) Example of fluvial channelized conglomerate facies association eroding into floodplain, intercalated sandstones and mudstones facies association, Korfiotissa Formation (0633503 4214660). (c) Block of freshwater marly limestones containing reworked seasonally banded tufa within Ano Pitsa Formation. The tufa blocks were probably eroded during high fluvial discharge from nearby palustrine marginal springs mounds, Xylokastro horst (0632590 4216336). (d) Detrital tufa fragments and pisoids in coarse-grained basal part of bedded detrital freshwater limestones with low angle cross-bedding, interpreted as lake margin environment. Ano Pitsa Formation, Xylokastro horst (0632590 4216336).

Well-sorted sandstones and conglomerates

This facies association comprises well-sorted and rounded medium to coarse sandstones and well-sorted, small-pebble conglomerates with a sheet-like geometry, quite unlike the Korfiotissa channelized conglomerates. They exhibit low angle trough cross-stratification and pebble imbrication.

The predominantly fine-grained facies association is indicative of seasonally wet floodplain environments and more continuously wet, lake-margin palustrine facies and fluvial-palustrine tufa stromatolites (Pedley, 1990; Alonso-Zara & Wright, 2010). It has similarities with the Valimi Formation further west (Rohais *et al.*, 2007a; Ford *et al.*, 2013; Hemelsdaël *et al.*, 2017). The gastropods are exclusively freshwater types. In situ tufa stromatolites are indicative of slow-flowing fluvial to lacustrine conditions, with intraclasts and reworked tufa blocks indicating periodic erosion by sustained river flow or flash flooding (braided model of Pedley, 1990). Incipient soil formation is indicated by weak vertisols and stage 1 pedogenic calcretes formed under seasonally wet and dry conditions. The thinner sandstones represent distal crevasse and sheet-flood deposits, with the lignites forming in marshy areas. As with the Korfiotissa Formation, the channelized conglomerates were deposited in vigorous fluvial channels. The finer well-rounded and well-sorted conglomerates suggest high-energy, lake shoreface-beach processes with fluvial detritus reworked by longshore drift.

Pellini Formation

The 400 m-thick Pellini Formation outcrops within a fault-bounded block, bounded by the Amphithea fault to the north and a set of sub-parallel, NE-SW-trending faults on the western slopes of the Sythas valley to the south (Fig. 2). Poorer quality exposures occur along the southeast dip-slope of the Amphithea horst (Fig. 2). Stratigraphic and structural relationships indicate that the

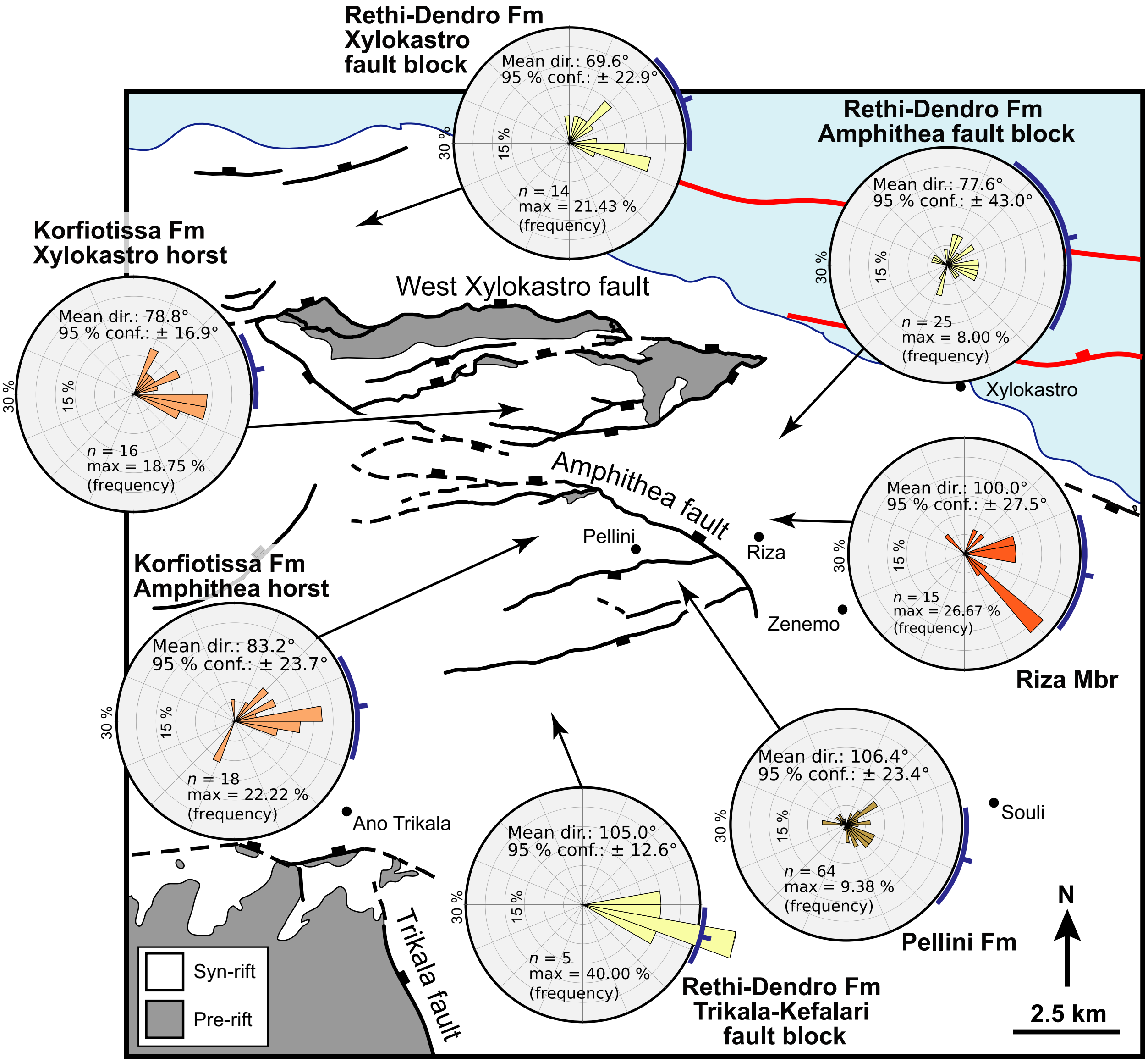

Fig. 5. Summary of palaeocurrent data from the Korfiotissa, Pellini and Rethi-Dendro formations for different structural domains within the study area. Simplified geological map with pre-rift Hellenide basement and syn-rift shown. Faults active post 0.8 Ma – red; older, inactive faults – black.

formation is younger than the Ano Pitsa Formation and older than the majority of the Rethi-Dendro Formation (Fig. 3a). The Pellini Formation comprises three facies associations: (a) sheet-like to channelized conglomerates and sandstones, (b) interbedded mudstones, marlstones and sandstones, and (c) intraclast-dominated and folded units.

Sheet-like to channelized conglomerates and sandstones

These buff to light brown coloured conglomerate and sandstone bodies have a range of geometries. Isolated, strongly erosive channels, 2–8 m thick, can extend laterally for 10–50 m. Laterally extensive sheets range in thickness from 3 to 15 m and may extend beyond the limits of exposure (>500 m) and comprise vertically and laterally amalgamated channel forms (Figs 3d and 6a, b). They are composed of fine-pebble conglomerates with medium to coarse sand matrix, with a maximum clast size of 15–20 cm. The base of scours and channels also contain large moulds of branches or trunks of trees. Beds, 0.5–2 m thick, tend to be massive, picked out by abrupt changes in grain size or intercalations of 10–30 cm-thick coarse to granular sandstone that define a crude, parallel to low angle stratification within the channel forms (Fig. 6b). The sandstone-dominated channels are filled with sharp-topped and sharp-based tabular beds 15–60 cm thick that are largely

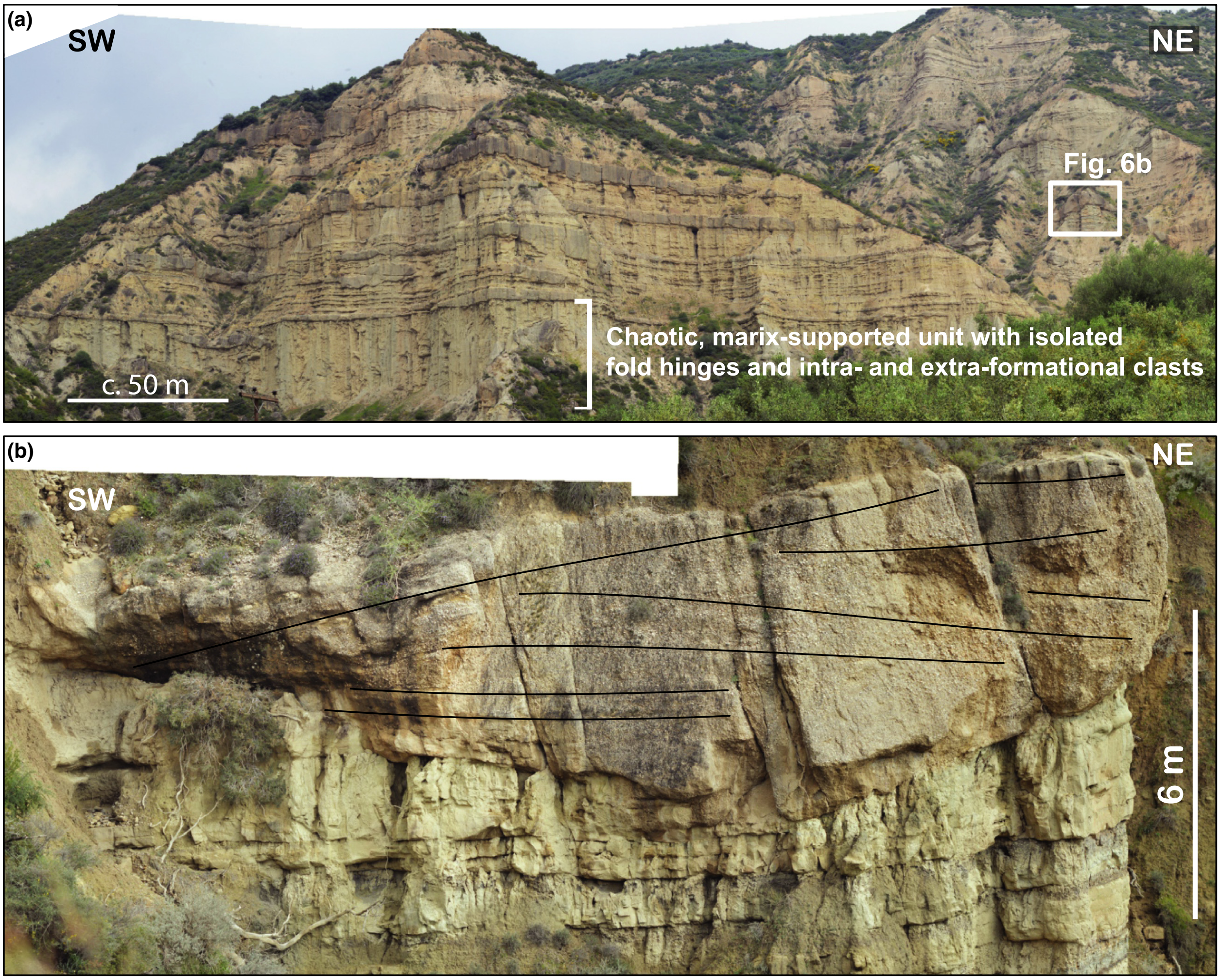

Fig. 6. Sedimentary characteristics of the Pellini Formation (see Fig. 2 for location). (a) Overview showing typical stratigraphic architecture of alternating sheet-like to channelized conglomerates and sandstones, and interbedded mudstones, marlstones and sandstones facies associations. Note the 25 m thick intraclast-dominated and folded unit (mass transport deposit) at the base of the section (0637608 4210588). (b) Detail of channelized conglomerates eroding into a succession of tabular medium to coarse sandstones interbedded with laminated mudstone. The inclined bedding in the conglomerate channel is interpreted to represent lateral accretion surfaces (0637300 4210935).

structureless, with floating granules and rare trough cross-bedding and planar lamination. As in the underlying formations, clast composition is dominated by limestone, with rare chert and green sandstone clasts derived from the pre-rift Pindos unit.

Interbedded mudstones, marlstones and sandstones

This predominantly fine-grained facies association forms laterally continuous intervals up to 10 m thick. They are composed of grey- to buff-coloured structureless mudstones and siltstones up to 1 m thick, white laminated marlstones up to 20 cm thick and 0.1–1 m-thick sharp-based, fine to coarse sandstones and small pebble conglomerates (Figs 3d and 6b). The thicker sandstone and conglomerate beds often have erosive bases with pebble lags and are generally structureless, whereas thinner sandstone beds have planar tops and bases, fine upward and have laminated to rippled tops. Macrofossils are restricted to rare thin-shelled gastropods scattered in sandstone and siltstone beds; locally bioturbation is developed. Plant material may be found concentrated along laminations and as rare beds <5 cm thick.

Intraclast-dominated and folded units

The third facies association is characterized by detached isoclinal folds and 1–2 m-thick thrusted sheets of mudstone, sandstone and conglomerate in a poorly sorted, coarse intraclast and exotic pebbly conglomeratic matrix

(Fig. 6a). It is most spectacularly developed at the base of the northern part of the Pellini Formation outcrops where the unit is >25 m thick (Fig. 6a).

The finer grained facies association is interpreted to represent sedimentation in a subaqueous environment, below storm wave base, subject to fluctuating energy conditions. The low diversity body fossils and local bioturbation suggest a non-marine, lacustrine environment. The mudstone and marlstone intervals are interpreted to represent deposition from distal, low-energy flows and hemipelagic fall-out. The thinly bedded sandstones displaying partial Bouma sequences of sedimentary structures imply deposition from dilute, waning turbidity currents (Bouma, 1962). The channelized sandstones and conglomerates are interpreted to represent sub-lacustrine channels and channelized lobe complexes, formed by high-energy gravity flows of varied character, from fully turbulent to laminar, and probably mostly hyperpycnal because of the ambient lacustrine conditions. The much-deformed facies association suggests major syn-sedimentary deformation and sediment remobilization in mass flows. These interpretations suggest the Pellini Formation was deposited in an overall lower slope to pro-delta depositional setting, somewhat similar in character to parts of the modern Gulf of Corinth (Papatheodorou & Ferentinos, 1993; Leeder *et al.*, 2002; McNeill *et al.*, 2005; Lykousis *et al.*, 2007; Sakellariou *et al.*, 2007; Bell *et al.*, 2008). Palaeocurrent data, together with the predominance of clasts sourced from the pre-rift Pindos unit, suggest a westerly source, most likely from either the Kyllini delta (Rohais *et al.*, 2007a), or the major fluvial system further west in the Kalavryta area (Ford *et al.*, 2013). Clast types preclude a Mavro, Evrostini or Ilias delta source as these all contain abundant metamorphic clasts.

Rethi-Dendro Formation and Riza Member

The Rethi-Dendro Formation was originally defined and mapped in badlands exposed to the north of the Xylokastro horst and, to the south and east, in the tributaries of the Fonissa and Sythas rivers (Koutsouveli *et al.*, 1989) (Fig. 2). It passes westward into the Aiges Formation (Rohais *et al.*, 2007a,b; Leeder *et al.*, 2012). We distinguish an informal Riza Member with coarser, brown-weathering successions in the Amphithea fault block (Fig. 2).

The Rethi-Dendro Formation is variable in thickness, 1500–1800 m in the hanging wall of the Amphithea fault and possibly over 3 km thick in the hanging wall of the Kyllini-Trikala-Kefalari fault (Fig. 2). It comprises repeated alternation of three main facies associations: (a) marlstones and siltstones, (b) sandstones and conglomerates, and (c) conglomerates (Fig. 7a).

Marlstones and siltstones

This fines-dominated association comprises white marlstones and light grey siltstones with thin sandstones and occasional conglomerate lenses (Figs 3e and 7b). It contains distinctive, mappable white marlstone-dominated units interbedded with centimetre-scale parallel beds of siltstone and very fine to medium sandstone with rippled tops (Figs 3e and 7a). Marlstone beds range from finely laminated to moderately bioturbated, with *Planolites* descending from the base of the coarser-grained beds. Both lithologies contain freshwater faunas; monotypic ostracods from the former and diatoms from the latter. The coarser beds have sharp, planar bases and grade upward into marlstones often with partial Bouma sequences of sedimentary structures. Conspicuous plant fragments also occur, with rare conglomerates in shallow lenses <1 m thick, extending laterally >15 m.

Sandstones and conglomerates

This association is dominated by fine to coarse sandstones, locally channelized, with subordinate conglomerates (Figs 3e and 7c, d) and is similar to that described from the Pellini Formation. Units up several tens of metres thick form laterally extensive sheets (>7 km) that internally may contain channelized sandstone bodies up to 4 m thick and with width/thickness ratios >50 (Figs 3e and 7c, d). Soft-sediment deformation in the form of horizons of isoclinal folds and thrusts, ball-and-pillow structures occur within this facies association. Clast types include not only a variety of limestone and chert with rare sandstones of Pindos unit provenance, but also plentiful metamorphics (quartzite and phyllitic schist) derived from a deeper nappe pile.

Conglomerates

Punctuating the Rethi-Dendro Formation succession are rare conglomerate bodies, 3–20 m thick, which extend laterally for up to 2 km. These are composed of laterally and vertically amalgamated lobes of conglomerates with clasts ranging in size from 1 to 15 cm. These bodies show evidence of soft-sediment deformation such as loading, sedimentary dike intrusions of underlying marlstone-rich deposits, and syn-sedimentary normal faulting.

Stratigraphic architecture is dominated by cyclicity of the coarse and fine facies associations on a scale of several tens of metres, giving tabular units that can be traced laterally over >5 km (Fig. 7a). Both of these facies associations may be involved in soft-sediment deformation occurring in intervals several tens of metres thick. As in the Pellini Formation, palaeocurrents are predominantly

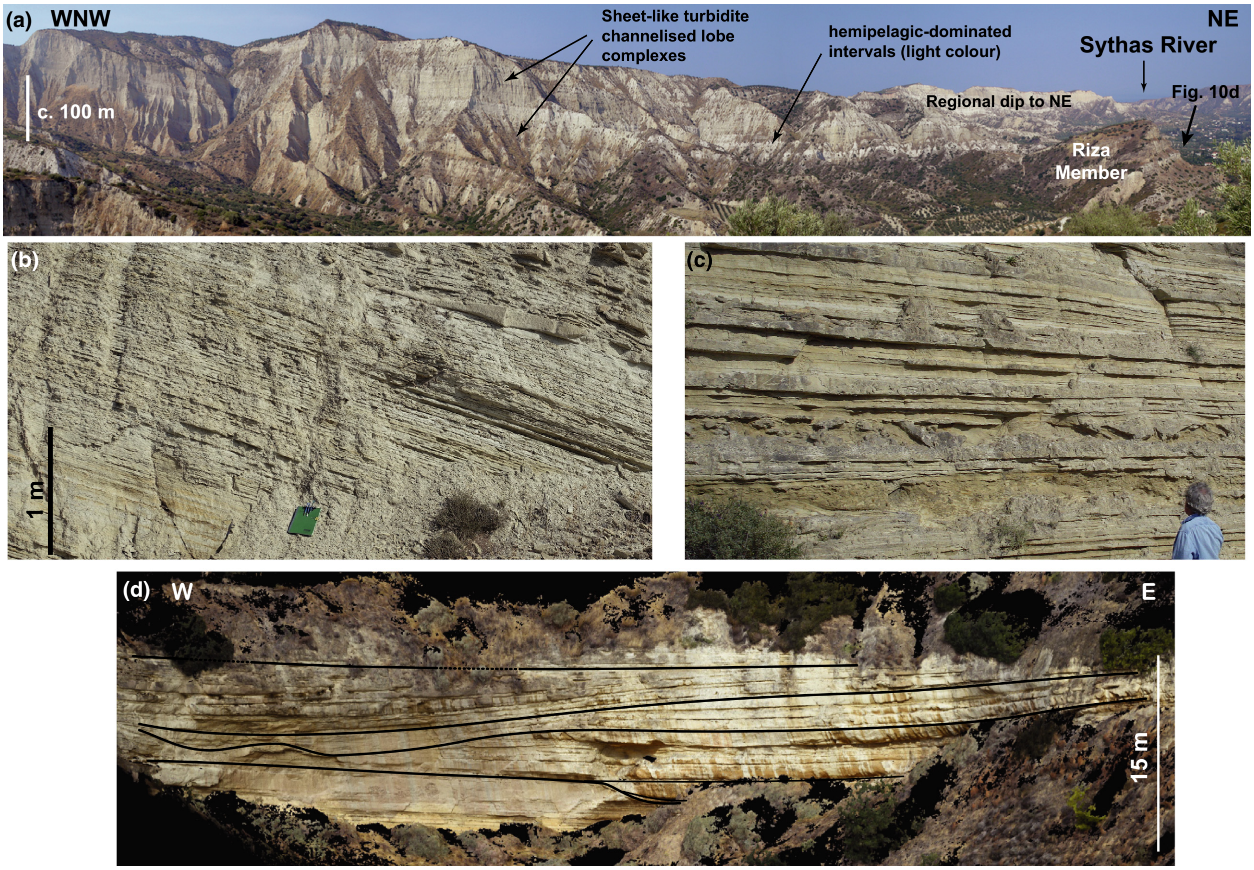

Fig. 7. Sedimentary characteristics of the Rethi-Dendro Formation (see Fig. 2 for location). (a) Large-scale view of the stratigraphy of the formation within the Amphithea fault block (W side of Sythas valley) showing tens of metre, sheet-like alternation of sandstone-rich and marl-dominated facies associations. (b) Marlstone and sandstone facies association (0640370 4209033). (c) Sandstone-dominated facies association with tabular bedded turbidites and thin intraformational slumps (0627472 4219503). (d) Digital outcrop model of channel complex composed of sandstone and conglomerate facies association of the Riza Member with the main erosive boundaries are highlighted. Field of view is 90 m (0638870 4212670). Digital outcrop model is based on a combination of LiDAR and photogrammetry.

towards easterly quadrants sub-parallel to fault strike, with azimuths to 70° in the Xylokastro fault block and to 78° and 105° in the Amphithea and Trikala-Kefalari fault blocks, respectively (Fig. 5). The Riza Member has a similar mean azimuth – to 100° (Fig. 5).

The Riza Member is up to 150 m thick (Fig. 3a) and comprises a series of conglomerate- and sandstone-rich units separated by marlstones and siltstones. The deposits in the basal part of the member are the coarsest, and consist of conglomerates and sandstones that form amalgamated sheets up to 3 m thick and extend laterally for at least several hundred metres. These sheets are interbedded with 2 m-thick units comprising laminated mudstones and sharp-based, rippled-top sandstones (Fig. 3e). The Riza Member also contains channel bodies over 100 m wide and 5–10 m thick (Fig. 7d) composed of the sandstone and conglomerate facies association. Examples of laterally accreted lenses, up to 5 m thick and extending laterally for up to 25 m, occur within the overall channelized forms.

The depositional environment of the Rethi-Dendro Formation fits broadly with a predominantly sub-lacustrine channel/lobe complex in the basin floor setting outlined for the Pellini Formation. However, the sedimentary clasts indicate provenance from a Hellenic nappe source that must include Tripoli limestone, Tyros basic volcanics and the Phyllites-Quartzites unit, i.e. a source in the nappe pile considerably deeper than the Pindos unit that sourced the older formations. This deeper provenance is shared by the Mavro and younger Evrostini and Ilias fan deltas in the west of the study area (Rohais *et al.*, 2007a; Leeder *et al.*, 2012) and, based on the palaeocurrent azimuths, it must be from these more proximal depositional systems that the majority of the Rethi-Dendro Formation sediment was derived. Erosively based and laterally accreted lenticular sandstone intervals represent deposits of sub-lacustrine meandering channel complexes with deposition taking place beneath vigorous turbidity underflows. The thicker conglomerate and massive sandstone beds may represent quasi-continuous flows. By way of contrast, the laterally extensive tabular beds were deposited under unconfined conditions as sub-lacustrine fan lobes. The poorly exposed fine-grained sediments that separate the coarser channel and lobe successions are probably deposited from decaying low-density underflows and by hemipelagic settling from the overlying water column. Soft-sediment deformation structures range from subaqueous slides and slumps to horizons displaying evidence for dewatering and liquefaction, possibly triggered by earthquakes. Rethi-Dendro Formation cyclicity defined by the stacking patterns of the coarse and fine facies associations may relate to autogenic fan lobe-switching, or to allogenic sediment supply variation or base-level changes in Lake Corinth related to climatic fluctuations – a subject of ongoing research.

Coarse-grained deltas, marine terraces and tufa deposits

Coarse-grained deltas occur in the study area; some are age-equivalent to the formations described here, whereas others unconformably overlie them. In addition, clastic-dominated shallow marine deposits and non-marine carbonates (mainly tufas) unconformably overlie the main mapped formations (Fig. 2).

Coarse-grained deltas

Uplifted and incised giant Gilbert-type fan deltas feature prominently along the western edge of the study area and have been studied by several workers (Ori, 1989; Rohais *et al.*, 2007a, 2008; Gobo *et al.*, 2014, 2015). They form a number of discrete delta complexes (the Kyllini, Mavro, Evrostini and Ilias deltas) that may exceed 1000 m in thickness. Coarse-grained fan delta deposits also occur in the south of the area, in the immediate hanging wall of the Trikala and Kefalari faults (Fig. 2). They form an aggradational to progradational delta complex up to 3 km in radius, here named the Kefalari delta (Figs 2 and 8a). The delta topsets are tilted to the south; foresets are several hundred metres high and are locally affected by growth faulting (Doutsos & Piper, 1990) (Fig. 8a).

Other coarse-grained deltaic deposits occur immediately to the north of the Kefalari delta, but have a dramatically different geometry, forming a staircase of delta terraces that decrease in elevation northward. This coarse-grained delta complex, here named the Kryoneri delta, progressively steps down in elevation from *ca.* 1000 to 700 m (Figs 2 and 8b). Between N-facing scarp-like steps in the top of the delta, the delta top has a terrace-like morphology and is generally planar and sub-horizontal, although it is locally incised by palaeovalleys, for example the NNW extension of the Stymfalia valley (Fig. 2). The base of the delta is an angular unconformity subcropped by tilted Rethi-Dendro Formation marls and turbidites. The elevation of the basal unconformity mimics the northward downstepping morphology of the delta top. Internally, individual delta terraces are markedly progradational with sub-horizontal to shallowly S-dipping topsets and foresets that dip up to 25° to the north and range in height from 50 to 200 m (Fig. 8b–d). There is an overall trend to progressively thinner foresets in the lower (younger) terraces. Overall the delta terraces have a sheet- to lobe-like planform, some with a radius of >5 km.

Marine terraces

Flights of marine terraces and shorelines unconformably overlying older Plio-Pleistocene rift sediments, mainly the Rethi-Dendro Formation, have been mapped from >600 m elevation to the modern coastline (Keraudren & Sorel, 1987; Armijo *et al.*, 1996) (Figs 2 and 8b). The terrace deposits have been interpreted as forming along wave-dominated shorelines overlying transgressive ravinement surfaces, with local fluvial influence (Collier, 1990; McMurray & Gawthorpe, 2000). Based on U-series dating of corals the terraces in the Corinth area, they have been correlated with glacio-eustatic highstands extending back to at least 400 Ka (Keraudren & Sorel, 1987; Collier, 1990; Armijo *et al.*, 1996; Turner *et al.*, 2010)

Tufa deposits

Tufas of Late Pleistocene to Holocene age are preserved as patches up to a few km^2 throughout the study area (Fig. 2). In almost all cases the tufa deposits rest unconformably on older sediments, usually Rethi-Dendro Formation marls or sandstones or their proximal equivalent conglomerate facies. The tufa at Zemeno is the most securely dated with a U-Th age of 89 +21/−15 ka, suggesting formation during late MIS 5 (Brasier *et al.*, 2010). Tufas on the valley slopes at Manna (Fig. 2) form a series of at least five flat-topped, perched, barrage and ramp deposits that developed as the Sythas valley deepened. The oldest deposit (undated) is 300 m above the valley floor, incised by the modern stream and karstified; it is also the biggest deposit being *ca.* 30 m thick and 50 m wide. The tufa at Elliniko, north of the West Xylokastro fault (Fig. 2), is unusual in that it overlies, and therefore post-dates, beach gravels of a marine terrace deposit, the base of which is at 414 m elevation. In general the tufas are perched spring-line deposits with cascade, tufa cone and, in some cases, paludal facies (Brasier *et al.*, 2010, 2011). In all cases these deposits represent spring-fed, valley slope or valley floor environments that developed as the modern river valley topography evolved. Continued

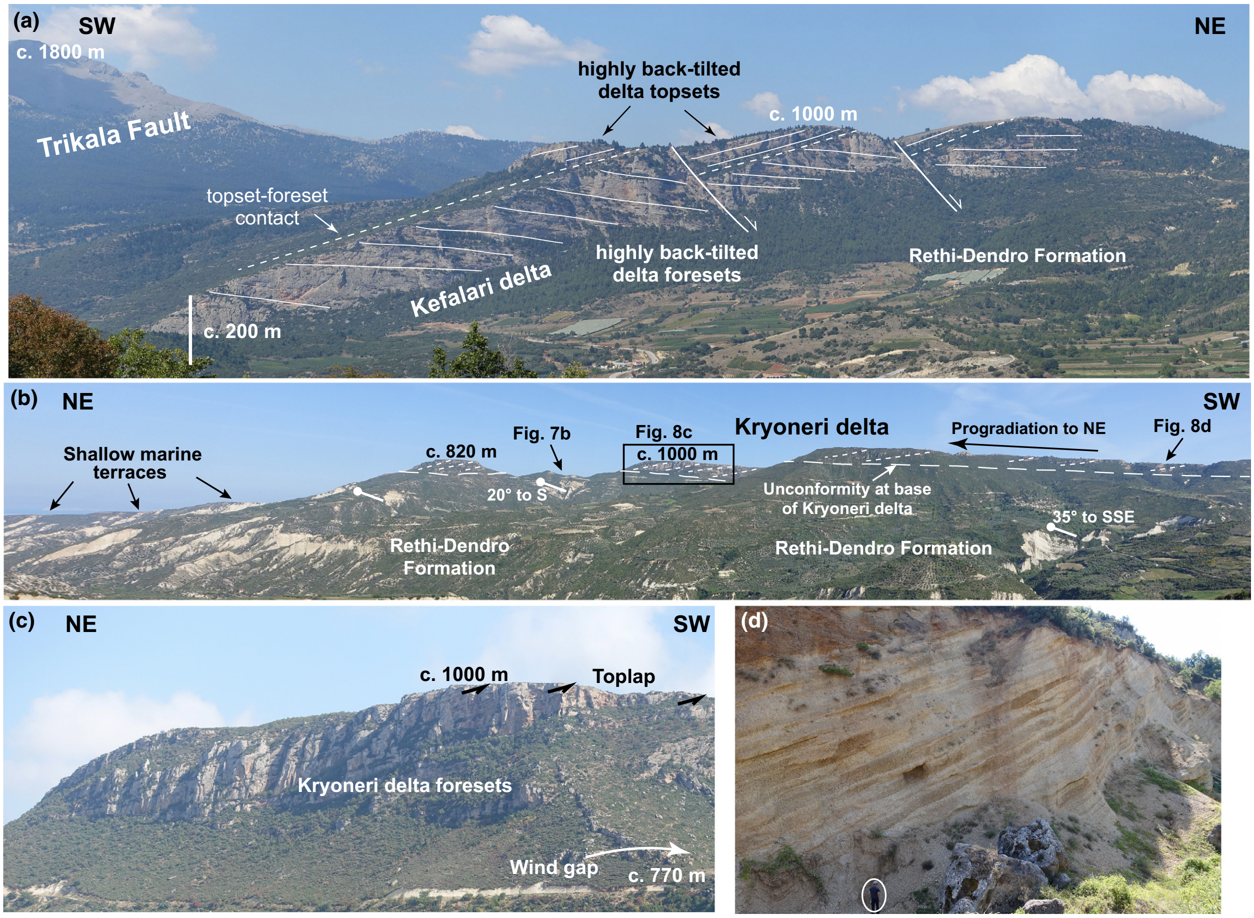

Fig. 8. Coarse-grained deltas and marine terraces (see Fig. 2 for location). (a) West side of the northern Stymfalia valley NE of the town of Kefalari. Topsets and foresets of the Kefalari delta are highly rotated (to S) in the hanging wall of the Trikala-Kefalari Fault. The hills to the SW are composed of pre-rift Hellenide units in the footwall of the Trikala Fault. (b) Coarse-grained Kryoneri delta unconformably overlying S- to SE-tilted Rethi-Dendro Formation along the E side of Sythas Valley. Note strongly progradational character of the Kryoneri delta capping the valley sides and shallow marine terraces at lower elevation (left of photo). (c) View of stratal geometry within the Kryoneri delta. Note lack of topsets and strongly progradational character. The top of the delta is a sub-horizontal topset surface which is itself incised (edge of incised valley [now a wind gap] just visible on right of photo). Main cliff is approximately 200 m high; location shown in (b). (d) Detail of foreset facies within the Kryoneri delta showing open-framework, clast-supported conglomerates with lenticular to lobate bedding geometry, dipping at up to 30°. Person circled for scale; location shown in (b).

incision and uplift has left the highest parts of these deposits incised by their own drainage, partially eroded and heavily karstified.

CHRONOSTRATIGRAPHY AND AGE RELATIONSHIPS

The discovery and dating of the Stamatakis ash towards the top of the Rethi-Dendro Formation exposures within the Amphithea fault block (Leeder *et al.*, 2012) is of major significance in constraining the chronostratigraphic evolution of the study area (Fig. 9) and of the Corinth rift as a whole. It provides one of only three sets of absolute ages within the syn-rift succession that are older than those associated with the Late Pleistocene terrace deposits. We use the ash to estimate the age of the base of the Rethi-Dendro Formation exposed in the Amphithea fault block. Using the thickness of the Rethi-Dendro Formation below the ash (800–1000 m) and a mean deposition rate similar to that determined from Late Pleistocene turbiditic/hemipelagic deposits from the modern central rift floor (Moretti *et al.*, 2004) gives an age of *ca.* 3.3 Ma (Fig. 9). Furthermore, as the 300–400 m-thick Pellini Formation underlies the Rethi-Dendro Formation, and applying the same approach, a minimum age for the base of the exposed Pellini Formation of *ca.* 3.6 Ma is suggested. This marks the advent of the lacustrine flooding event (the 'Great Deepening' event of Leeder *et al.*, 2012) that separates the Pellini Formation from underlying fluvial to lake margin environments of the Korfiotissa and Ano Pitsa formations, for which we currently have no age constraints (Fig. 9).

Combining these age estimates with provenance and palaeocurrent information allows us to propose timing relationships for the sediment sources feeding the Pellini and Rethi-Dendro formations. Palaeocurrent azimuths are similar in the two formations: dominant flow was to the east, axial to the main rift structure (Fig. 5). This suggests sediment sourced from catchments feeding the major coarse-grained deltas in the SW and W of the study area and/or from the major Kalavryta fluvial system further west. Rohais *et al.* (2007a) describe the Kyllini delta as containing only a few metamorphic clasts. Thus, we interpret the Pellini Formation to have been sourced from either a N-flowing Olvios river, via an active Kyllini delta, or a more distal, Kalavryta fluvial source to the west that lacks metamorphic clasts (Fig. 9). The metamorphic-rich Rethi-Dendro Formation in the Amphithea fault block suggests that by approximately 3.3 Ma the Phyllites-Quartzites unit was being eroded in the rift shoulder and that sediment was supplied by a N-flowing Olvios river via the Mavro delta into Lake Corinth where the Rethi-Dendro Formation was being deposited (Leeder *et al.*, 2012) (Fig. 9).

The Rethi-Dendro Formation in the Xylokastro fault block passes westward into the Aiges Formation and the Ilias and Evrostini deltas (Leeder *et al.*, 2012). These form part of a suite of now uplifted early Pleistocene deltas, including Kerinitis, Vouraikos, Planatos and Prioni, that formed in the hanging wall of the Pyrgaki-Mamoussia-Valimi and West Xylokastro faults. We have no direct age constraints on the Rethi-Dendro Formation in the hanging wall of the West Xylokastro fault block, but dating of syn-tectonic calcite cements from the fault zone suggests the West Xylokastro fault was active about 1 Ma (Flotte *et al.*, 2001; Causse *et al.*, 2004). Palynological data from the Kerinitis and Vouraikos deltas to the west suggests deposition occurred between 1.8 and 0.7 Ma (Malartre *et al.*, 2004; Backert *et al.*, 2010; Ford *et al.*, 2013), significantly younger than the Rethi-Dendro Formation in the Amphithea fault block to the SE (Fig. 9).

Further chronological constraints are provided by the Late Pleistocene marine terraces that unconformably overlie the Rethi-Dendro Formation and are interpreted to extend back to older than MIS 15,

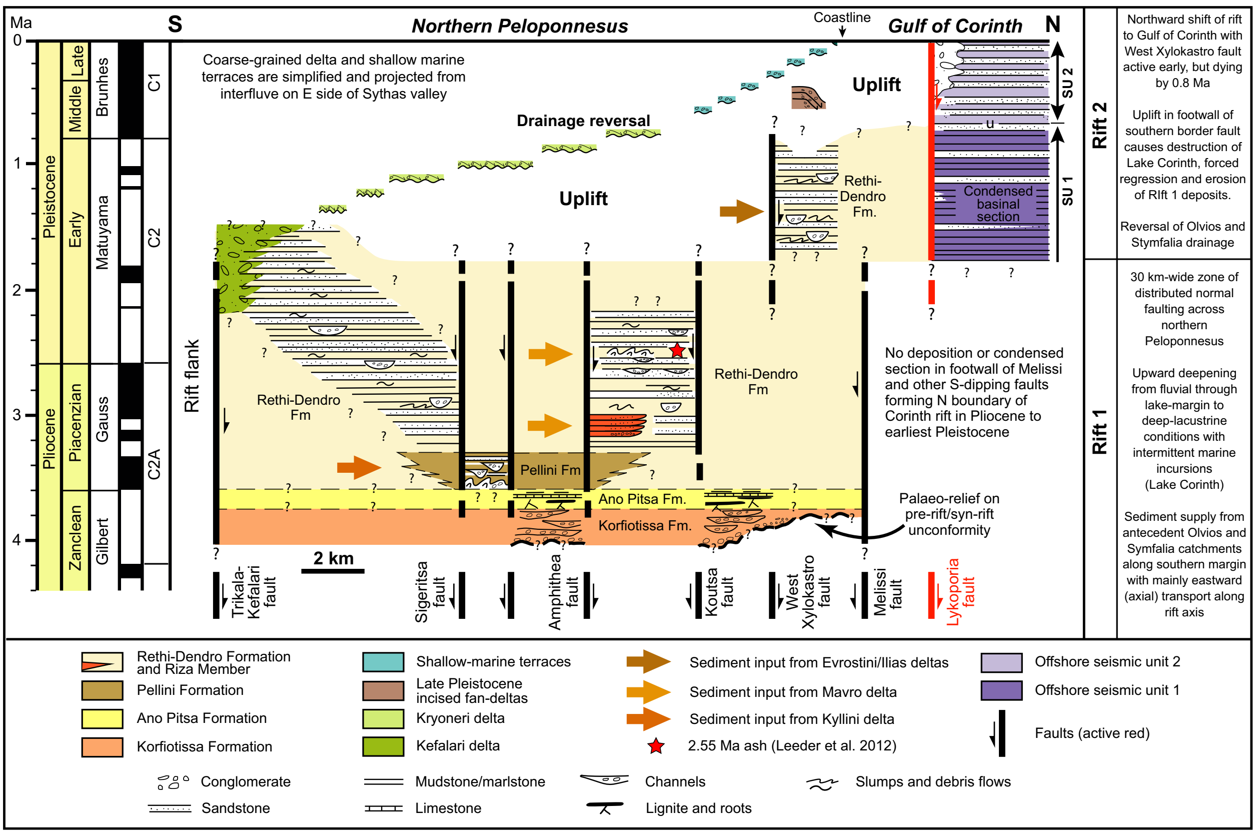

Fig. 9. N-S swath chronostratigraphic section showing proposed age-model and provenance for the central onshore Corinth rift together with correlation with offshore (based on Nixon *et al.*, 2016). Location in space and time of lithology and sedimentary bodies shows present-day preservation and exposure of the various units. Details of present erosion level omitted for clarity. Faults are named along bottom of diagram. See text for full discussion.

approximately 0.6 Ma (Armijo *et al.*, 1996) (Fig. 9). The Kryoneri coarse-grained delta terraces extend further south and to higher elevation (up to 1000 m) and are therefore older than the marine terraces. Extrapolating the uplift rates based on the dated marine terraces suggests an age of >700–800 ka for the Kryoneri coarse-grained delta terraces, although we have no direct evidence that these terraces are marine in origin and thus have no control on the sea- or lake-level they built into (Fig. 9). Such an old age for the Kryoneri delta is supported by dated paludal and cascade tufa capping terrace deposits further east around Nemea (Fig. 1). These tufas are older than 600 ka and probably around 1 Ma based on preliminary attempts at U-Pb isotopic analyses (Brasier *et al.*, 2011). These estimates suggest that the Kryoneri delta may be partially time-equivalent to the giant fan-deltas in the west (e.g. Kerinitis, Vouraikos deltas; Malartre *et al.*, 2004; Rohais *et al.*, 2007a,b; Backert *et al.*, 2010; Ford *et al.*, 2013, 2016).

STRUCTURE

In the study area, major inactive normal faults typically form E-W striking segments between 5 and 15 km long, with fault-plane dips of 35–70° (Figs 2 and 10). Faults with the largest present-day displacement (>1 km) dip northwards and have pre-rift Hellenide basement rocks exposed in their immediate footwall. These N-dipping faults are the West Xylokastro fault, the Amphithea fault and the Kyllini-Trikala-Kefalari faults (Fig. 2). Together with the S- to SE-dipping Koutsa and Sigeritsa faults they define the structural units of the Xylokastro fault block, Xylokastro horst, Amphithea fault block, Amphithea horst and Trikala-Kefalari fault block (Fig. 2). The faults that are currently active and define the present day southern border fault of the Gulf of Corinth lie just offshore, north of the mapped area (Fig. 2).

West Xylokastro fault, Xylokastro fault block and Xylokastro horst

The West Xylokastro fault is 20 km long and has generated steep topographic gradients and significant footwall relief, >1100 m at its centre. It has an overall zig-zag trace, with three longer, E-W-striking segments up to 8 km long, linked by shorter (<1.5 km), NW-SE-striking faults (Fig. 2). The fault segments have dips ranging mainly from 50 to 70°, with predominantly dip-slip displacement (Figs 2, 10 and 11a).

The Xylokastro fault block, located in the hanging wall of the West Xylokastro fault, exposes predominantly ESE-dipping Rethi-Dendro Formation unconformably overlain by shallow-marine terrace deposits, with spring-related tufa deposits near the village of Elliniko, and locally incised by coarse-grained deltas (e.g. Kamari delta at the mouth of the Fonissa gorge (McMurray & Gawthorpe, 2000)) (Fig. 2). The fault block is up to 5 km wide and continues offshore where it is bounded to the north by the offshore, N-dipping Lykoporia fault (Taylor *et al.*, 2011; Nixon *et al.*, 2016) (Fig. 2). Although the overall structural dip within the fault block is to the ESE, northerly dips, up to 25°, occur in the immediate hanging wall of the West Xylokastro fault, defining a N-dipping faulted monocline. North-dipping monoclinal folding and minor faulting of the Rethi-Dendro Formation is also locally developed along the northern most coastal exposures.

The Xylokastro horst has an elongated, E-W lenticular shape in map view. Pre-rift Hellenide basement occurs along the northern margin of the horst, in the footwall of the West Xylokastro fault (Fig. 2). The southern margin is bounded to the east by the Koutsa fault and by the Vryssoules fault in the southwest (Fig. 2). These faults downthrow younger Rethi-Dendro Formation of the Amphithea fault block in their hanging wall. Although the horst has a gentle southerly tilt, a narrow, elongated intra-horst graben containing the Ano Pitsa Formation occurs along the crest of the horst.

Amphithea fault, Amphithea fault block and Amphithea horst

The north-dipping (50–60°) Amphithea fault has an estimated minimum throw of at least 1 km. The dip-slip fault defines the southern edge of the Amphithea fault block, with the Amphithea horst in its immediate footwall (Figs 2 and 10). East of the Sythas valley, it rapidly loses displacement along a zone of minor north-dipping faults with rapid dip changes.

The Amphithea fault block in the hanging wall of the Amphithea fault, has a funnel-shaped planform, tapering westward from over 5 km to <500 m wide (Fig. 2). The fault block exposes spectacular cliff sections of N- to NE-dipping Rethi-Dendro Formation unconformably overlain by a staircase of shallow-marine terrace deposits (Figs 2 and 11b). The monoclinal geometry of Rethi-Dendro Formation bedding across the Amphithea fault along the eastern side of the Sythas valley, suggests that the Amphithea fault was active during deposition of the Rethi-Dendro Formation, probably upward-propagating to create a syn-sedimentary forced-fold (e.g. Gawthorpe *et al.*, 1997) (Fig. 11b). We interpret the overall N- to NE-dips within the Amphithea fault block to be due to a syn-depositional tilting in the hanging wall of a major, now-buried, S-dipping normal fault, the Melissi fault, located along the present-day coastline of the Gulf of Corinth (Figs 2 and 11b). This fault also explains exposures

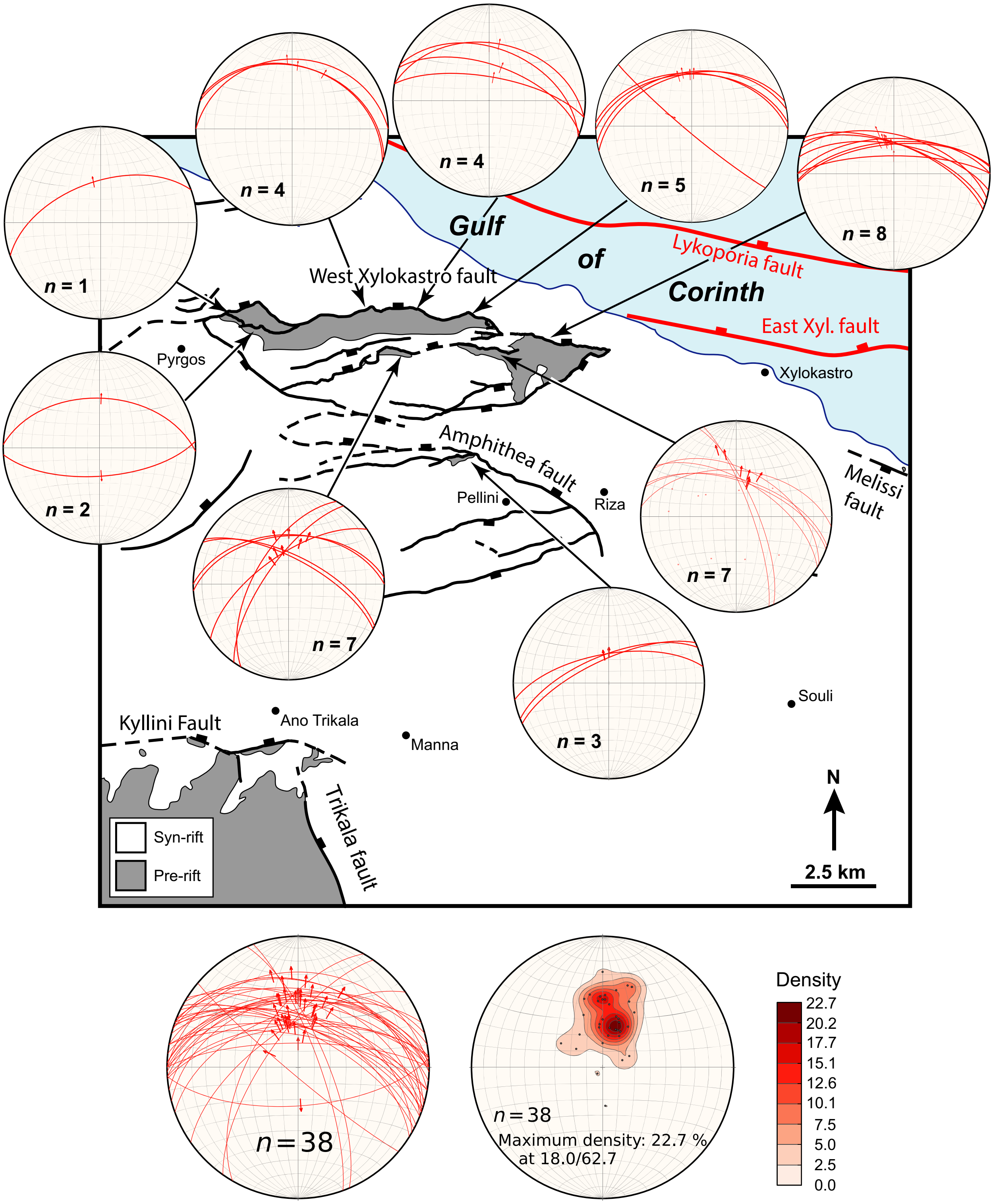

Fig. 10. Summary of fault planes and striations on major exposed normal faults (lower hemisphere, equal area plots). Bottom left – summary of fault dip and fault striation data. Bottom right – density plot of fault striations, indicating mean slip vector 62° to 018. Plots created with OpenStereo software (http://www.igc.usp.br/?id=391).

of pre-rift Mesozoic limestones at the coastal town of Melissi as part of the footwall of the fault (Skourtsos *et al.*, 2016).

The lozenge-shaped Amphithea horst in the footwall of the Amphithea fault has bedding dips within the horst that are generally 10–25° to the SSE (Fig. 2). It is cored by

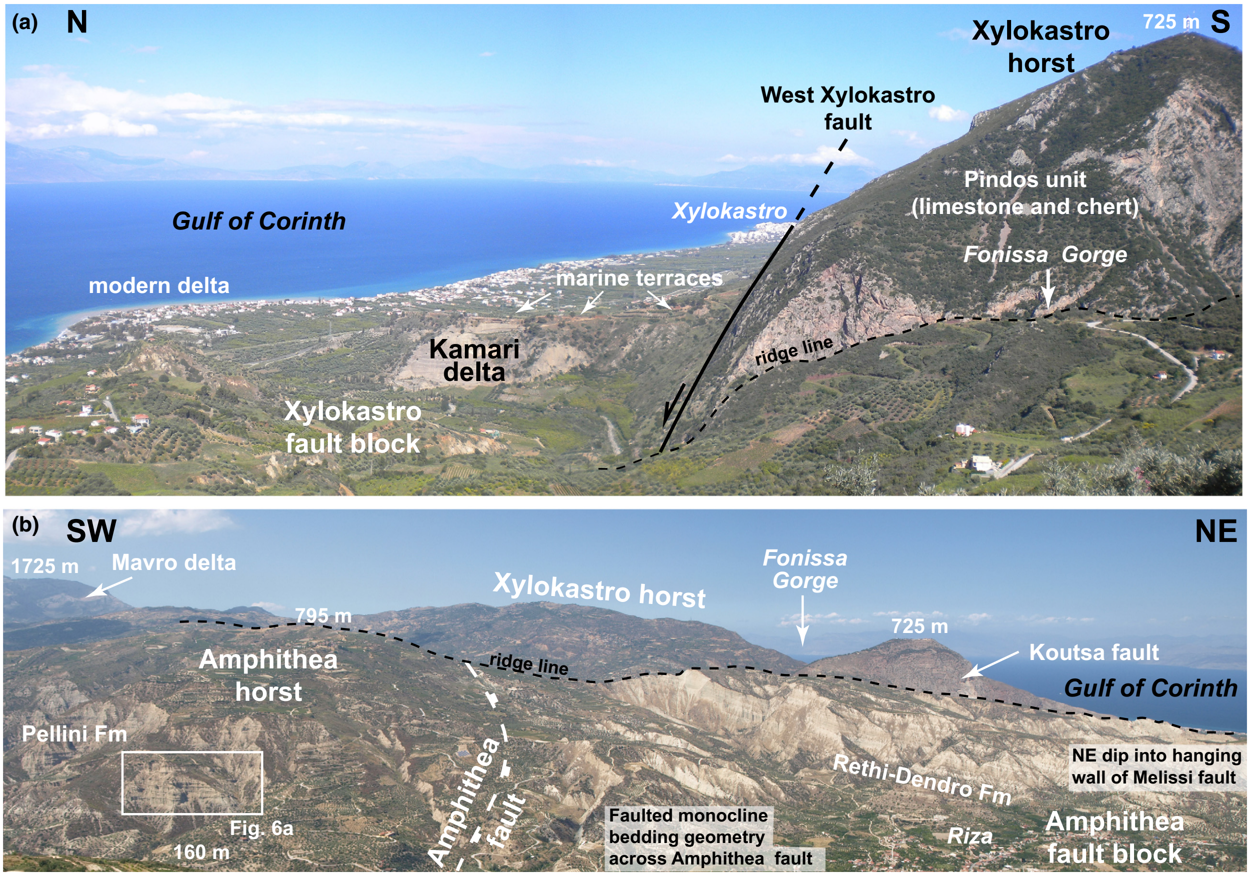

Fig. 11. Structural and stratigraphic relationships from different structural domains within the study area (see Fig. 2 for location). (a) View east along the easternmost segment of the West Xylokastro fault (Kamariotiko segment) showing Pindos unit limestones and cherts in the footwall (Xylokastro horst), with Late Pleistocene deltaic (Kamari delta) and shallow marine deposits unconformably overlying Rethi-Dendro Formation (covered) in the hanging wall (Xylokastro fault block). (b) West side of the Sythas valley overlooking the town of Riza showing monoclonal geometry of bedding in the hanging wall of the Amphithea Fault. The overall NE dip of bedding in the Amphithea fault block, interpreted to be due to syn-depositional tilting into the immediate hanging wall of the S-dipping Melissi Fault. The crest of the Xylokastro horst forms the skyline and the Mavro delta can be seen on the top left. Sigeritsa and other NE-SW-striking faults are not shown for clarity.

pre-rift Pindos unit limestones unconformably overlain by the Korfiotissa and Ano Pitsa formations. To the east the bounding Sigeritsa fault has an estimated throw of >300 m.

Trikala-Kefalari fault block

South of the Amphithea horst the Rethi-Dendro Formation of the Trikala-Kefalari fault block dips southwards into the hanging wall of the major Kyllini-Trikala-Kefalari fault (Fig. 2). This comprises the E-W-striking Kyllini and Kefalari faults linked by the NNW-SSE-striking Trikala fault. Estimated maximum throw is >3 km. The immediate hanging wall of the Kefalari fault comprises highly back-tilted coarse-grained deltas; the Kefalari delta (Fig. 8a), whereas the footwall exposing the whole suite of pre-rift Hellenide nappes in the northern Peloponnesus, from the topmost (Pindos) to the lowest (Phyllites-Quartzites). Fault surfaces are poorly exposed and preserved, so fault kinematics are poorly constrained.

TECTONO-SEDIMENTARY EVOLUTION OF THE CORINTH RIFT

We integrate our new sedimentary, structural and age information from the central onshore rift with published onshore and offshore data to develop a coherent view of the evolution of the Corinth rift as a whole (Figs 12 and 13). In doing so, we attempt to reconcile differences in age assignment, correlation and timing of activity on major structures. At a whole-rift scale we recognize two main rift phases:

Rift 1, from 5.0–3.6 to 2.2–1.8 Ma, saw extension distributed across the northern Peloponnesus and the Corinth and Megara basins in the east.

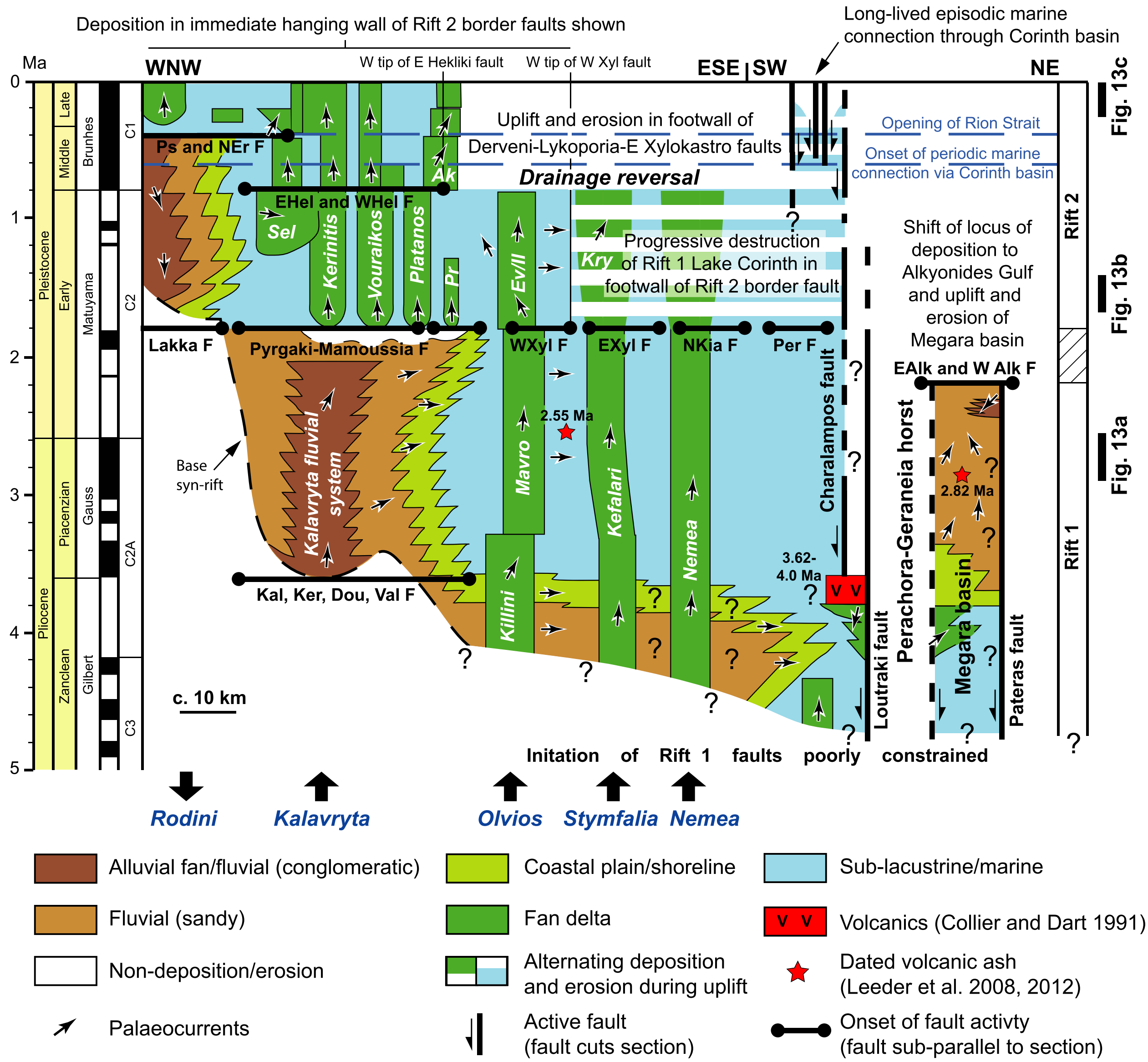

Fig. 12. The WNW-ESE to NE-SW swath chronostratigraphic section along the northern Peloponnesus and Corinth and Megara basins. Details of footwall erosion and terraces are omitted for clarity. Location of major drainage catchments shown with block arrows at base of figure. Western rift is modified after Ford *et al.* (2016) and Hemelsdaël *et al.* (2017); central rift – this study and Leeder *et al.* (2012); Corinth basin based on Collier & Dart (1991) and Megara basin after Bentham *et al.* (1991) and Leeder *et al.* (2008). Delta abbreviations – Ak, Akrata; Ev/Il, Evrostini/Ilias; Kry, Kryoneri; Pr, Prioni; Sel, Selinous. Selected fault names in bold; abbreviations – EAlk and WAlk F, East and West Alkyonides faults; EHel and WHel F, East and West Heliki faults; EXyl F, East Xylokastro fault; Kal, Ker, Dou, Val F, Kalavryta, Kerpini, Doumena and Valimi faults; NKia F, North Kiato fault; Per F, Perachora fault; Ps and NEr F, Psathopyrgos and Neo Erineos faults; WXyl F, West Xylokastro fault.

Rift 2, from 2.2–1.8 Ma to present, saw a dramatic northward shift in the locus of rifting to become largely coincident with the modern Gulf of Corinth.

Northward migration of faulting has been widely noted in previous studies of the Corinth rift, and our two phases of rift development correspond approximately to those recognized in the late 1980s and early 1990s in the west-central and eastern parts of the rift (Ori, 1989; Bentham *et al.*, 1991; Leeder *et al.*, 1991; Dart *et al.*, 1994) and from more recent work in the west-central rift (Rohais *et al.*, 2007a; Ford *et al.*, 2013). Our two-stage subdivision captures the major changes in rift development and recognizes that the rift structure evolved during each phase, due to the growth, linkage and death of normal faults and interaction with adjacent rift basins such as the Patras rift to the west. We consider northward and westward migration of activity over the last 0.8 Myr (Ford *et al.*, 2013,

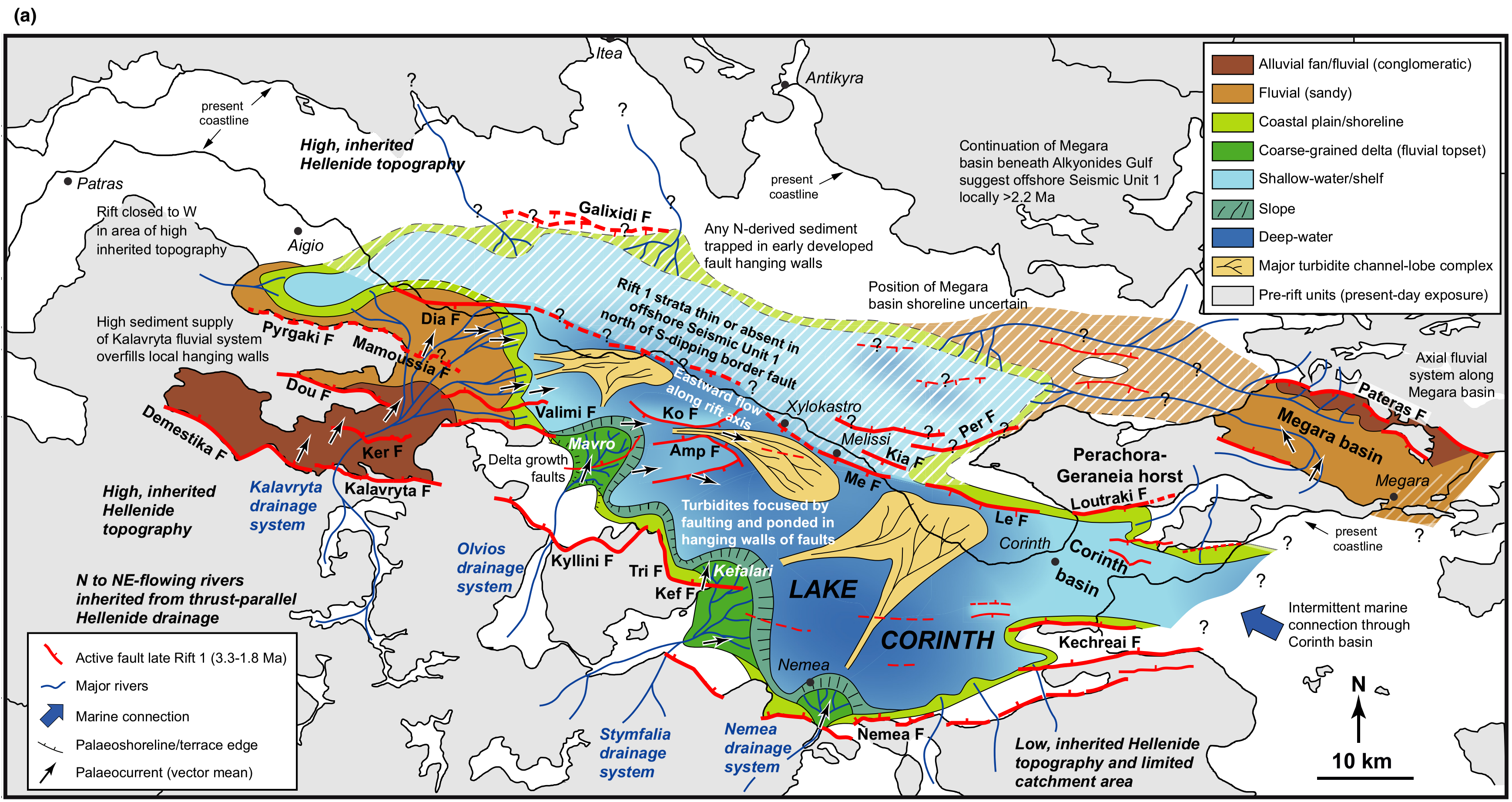

Fig. 13. Palaeogeographic and tectono-sedimentological evolution of the entire Corinth rift. (a) Late Rift 1, late Pliocene/Early Pleistocene. (b) Early Rift 2, Early to Middle Pleistocene. Delta abbreviations – Ev/Il, Evrostini/Ilias; Ker, Kerinitis; Pl, Platanos; Pr, Prioni; Sel, Selinous; Vou, Vouraikos. (c) Late Rift 2, Late Pleistocene. See text for a full discussion. Translucent colours and white diagonal shading represent areas of highest uncertainty. Fault names in bold; abbreviations – AK F, Ano Kastritsi fault; Amp F, Amphithea fault; Dia F, Diakofto fault; Dou F, Doumena fault; EAlk F, East Alkyonides fault; EXyl F, East Xylokastro fault; Her F, Heraion fault; Kef F, Kefalari fault; Ker F, Kerpini fault; Kia F, Kiato fault; Ko F, Koutsa fault; Le F, Lechion fault; Lyk F, Lykoporia fault; Me F, Melissi fault; Naf F, Nafpaktos fault; NKia F, North Kiato fault; Pan F, Panachaikon fault; Per F, Perachora fault; Ps F, Psathopyrgos fault; Psa F, Psatha fault; Tri F, Trikala fault; WAlk F, West Alkyonides fault; WPan F, West Panachaikon fault; WXyl F, West Xylokastro fault.

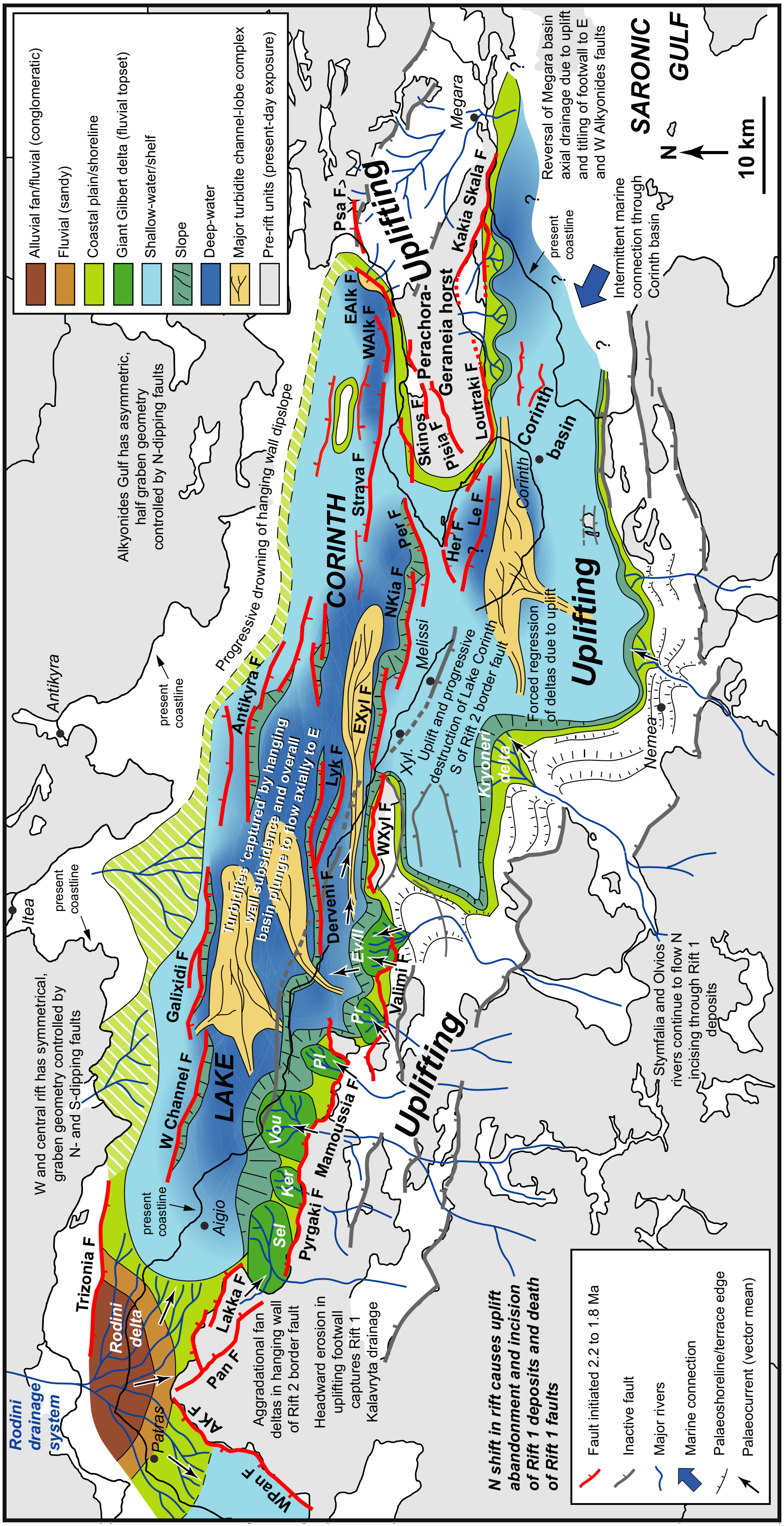

Fig. 13b. Continued.

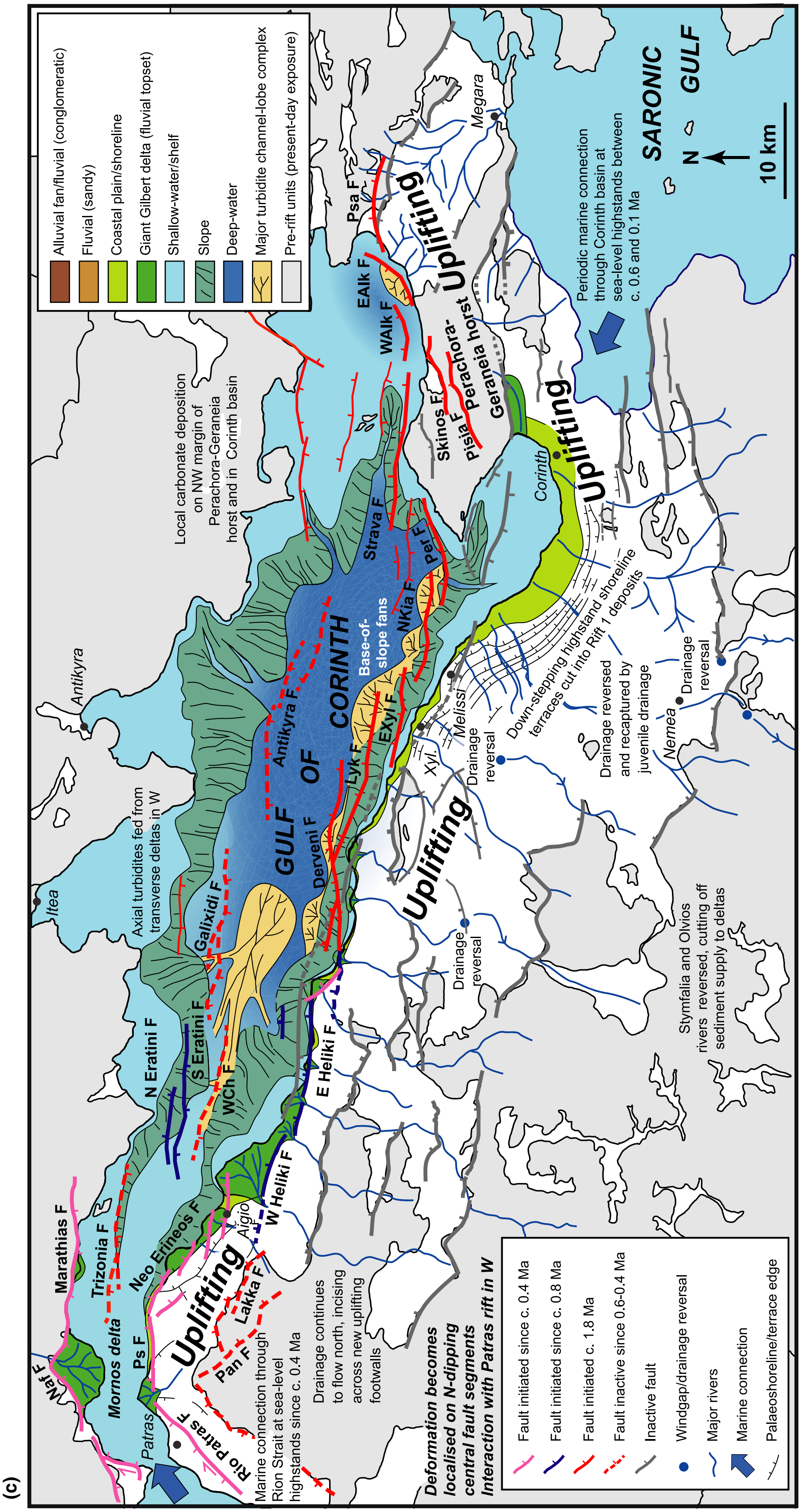

Fig. 13c. Continued.

2016) (Figs 12 and 13) to reflect fault interaction rather than representing discrete, basin-wide phases of rifting. During our two rift phases there were significant palaeoenvironmental changes, including marine incursions, changes in water-body dynamics (lacustrine hyperpycnal vs. marine hypopycnal), and climate-induced changes in sediment flux.

Rift 1: from 5.0–3.6 to 2.2–1.8 Ma

The timing of rift initiation is poorly constrained due to the isolated nature of exposures of earliest syn-rift sediments, the vagueness of relative chronologies provided by non-marine fossils, and the paucity of intercalated volcanics that might yield radiometric dates (Figs 12 and 13a). Early workers suggested post-Miocene rift initiation, perhaps between 4 and 5 Ma (Keraudren & Sorel, 1987; Ori, 1989; Doutsos & Piper, 1990), and later radiometric results from within the rift infill confirm that these suggestions are of the right order. In the east, >800 m of fluvio-lacustrine sediments in the Corinth basin occur beneath calc-alkaline lavas dated at 3.62 ± 0.18 and 4.00 ± 0.40 Ma (Collier & Dart, 1991). In the Megara basin, palaeomagnetic results tied to the precisely dated Pagae ash (2.82 ± 0.06 Ma) suggest that the kilometre-thick basin fill there must extend well into the Gilbert reversed chron between 5.89 and 3.58 Ma (Leeder *et al.*, 2008). As discussed in this paper, in the central rift at least 800 m of fluvial to lake shoreline sediments underlie the prominent lacustrine flooding estimated to have occurred around 3.6 Ma. Further west, magneto- and bio-stratigraphic results, unconfirmed by radiometric dating, suggest the onset of syn-rift sedimentation occurred around 3.6 Ma (Hemelsdaël *et al.*, 2017). These data may thus indicate some diachroneity in the onset syn-rift sedimentation, with rifting perhaps starting earlier in the east than the west.

Rift 1 was mainly located south of the present-day Gulf of Corinth in a 20–30 km-wide zone of distributed normal faulting, with both N- and S-dipping normal faults that define 3–8 km-wide tilted fault blocks (Fig. 13a). The southern rift margin was formed by a series of N-dipping normal faults (e.g. Kalavryta, Kyllini, Kefalari, Nemea faults) and the northern margin by a co-linear series of S-dipping normal faults (e.g. Diakofto, Melissi faults), giving the rift a graben-like form (Fig. 13a). The faults along the northern margin are now cross-cut by younger, N-dipping faults of Rift 2 and are partly buried by younger deposits. However, their importance is indicated by the northward dipping and thickening of Rift 1 deposits such as the Rethi-Dendro Formation in the Amphithea fault block (this study), and the Ladopotamos Formation in the Pyrgaki-Mamoussia fault block (Ford *et al.*, 2013). Further east, offshore seismic data shows S-dipping normal faults (Kiato and Lechion faults; Fig. 13a) with N-dipping early syn-rift growth wedges thickening into their immediate hanging walls (Charalampakis *et al.*, 2014). North of this, Rift 1 sediments were either not deposited or preserved (Nixon *et al.*, 2016), or they are thin and pinch out northwards, forming the lowermost part of the oldest (undated) offshore stratigraphy of Seismic Unit 1 (Nixon *et al.*, 2016). In the eastern part of the rift the Perachora-Geraneia horst splits the rift into two arms, the Megara basin to the north, bounded along its NE side by the Pateras fault, and the Corinth basin to the south, bounded by the Lechion and Loutraki faults to the north, and the Kechriae fault to the south (Fig. 13a).

Fault growth and syn-rift sedimentation during Rift 1 took place on a topographic template inherited from the Hellenide mountain belt, with marked regional and local topographic variations and well-established catchments and river systems (Ford *et al.*, 2013). Palaeotopography was highest in the west, declining eastwards like the present-day topography, and exerted a first-order control on the distribution of gross depositional environments along the rift – largely subaerial where topography was highest in the west and sub-lacustrine where topography was lower in the east. The eastward plunge of the palaeotopography also had a major effect on sediment transport within the rift axis, which was dominantly to the east during Rift 1. Superimposed on this regional palaeotopography was local antecedent drainage orientated sub-parallel to Hellenide folds and thrusts (i.e. NNE-SSW to NNW-SSE). The antecedent drainage formed palaeovalleys several hundred metres deep (Ford *et al.*, 2013; Hemelsdaël *et al.*, 2017), with margins strongly controlled by structure and lithological heterogeneity in the pre-rift Hellenide units.

Along the southern rift hinterland, four major N- to NE-flowing inherited drainages are recognized: Kalavryta, Olvios, Stymfalia and Nemea (Fig. 13a). We speculate that S-flowing rivers may have also drained the relatively high topography to the NW of the rift during Rift 1 (palaeo-Eratini and Itea rivers?), but that this sediment was largely trapped by local fault-controlled depocentres (e.g. offshore Galaxidi fault), and did not reach as far south as the main Rift 1 depocentre (Fig. 13a). In the east of the rift, lower inherited topography and limited hinterland catchment area, due to the proximity of the Argos Gulf to the south, restricted sediment supply from the southern rift margin. The palaeo-Perachora-Geraneia horst acted as a significant sediment source to both the Corinth and Megara basin as documented by a high proportion of serpentinite clasts, derived from ophiolites within the Pelagonian basement unit exposed on the horst (Bentham *et al.*, 1991; Collier & Dart, 1991) (Fig. 13a).

To the west the rift was probably closed to the Ionian Sea (the Patras rift having yet to form), with only intermittent marine connection to the SE to the palaeo-Saronic Gulf through the Corinth basin (Fig. 13a). Shallow lacustrine conditions were first established in the east in the Corinth basin before 3.6–4.0 Ma (Collier & Dart, 1991) and in the Megara basin before 3.6 Ma (Bentham *et al.*, 1991; Leeder *et al.*, 2008) (Fig. 12). Early syn-rift fluvial deposits overlying pre-rift units exposed in the central (this study) and western parts of the rift (Rohais *et al.*, 2007a; Ford *et al.*, 2013; Hemelsdaël *et al.*, 2017) suggest a major E-flowing fluvial system running axially along the main Rift 1 depocentre, sourced from the southern rift shoulder. Data from the Kalavryta system indicates high sediment flux and a fluvial system that was capable of filling local, fault-controlled accommodation to generate downstream facies and grain size changes that spanned several fault blocks and occurred over a length-scale >50 km (Hemelsdaël *et al.*, 2017) (Fig. 13a). The E-flowing axial fluvial system was progressively drowned and backstepped to the west (Kalavryta source) and to the south (Olvios, Stymfalia and Nemea sources) during the growth of Lake Corinth (Fig. 12). These southerly sediment sources subsequently became the sites of point-sourced coarse-grained deltas deposited in the hanging wall of the southern border fault (e.g. Kyllini and Kefalari deltas [Rohais *et al.*, 2007a; this study]) (Figs 12 and 13a). Our synthesis and revised age-model suggest that Lake Corinth was established over most of the main Rift 1 depocentre by approximately 3.6 Ma. Much of the rift from this time onwards was underfilled and sediment starved, characterized by deep-water hemipelagic and turbidite deposits (e.g. Pellini and Rethi-Dendro formations) typical of rift climax conditions (Prosser, 1993) (Fig. 13a).

Deltas at the western end of Lake Corinth, associated with the Kalavryta system shoreline, have clinoform heights of up to a few tens of metres (Rohais *et al.*, 2007a; Ford *et al.*, 2013), and we interpret this to reflect low axial gradients associated with the regional eastward plunge of the palaeotopography and along-strike displacement gradients of the active faults. In contrast, the major coarse-grained deltas in the hanging wall of the southern border fault (e.g. Kyllini and Kefalari deltas) have foresets up to several hundred metres high, and form aggradational to progradational packages hundreds of metres thick. A key control on the water depth these deltas built into was high subsidence in the immediate hanging wall of the Rift 1 southern border fault. Some of the deltas exploited relay ramps as entry points into the rift: for example, the palaeo-Stymfalia drainage exploited the segment boundary between the Kefalari and Nemea faults (Fig. 13a). The deltas were also subject to growth faulting, with major listric faults and associated roll-over hanging wall anticlines (Rohais *et al.*, 2007a). These coarse-grained deltas supplied powerful hyperpycnal turbidity currents that formed channel and lobe complexes within Lake Corinth (Pellini and Rethi-Dendro formations) (Fig. 13a).

The turbidite depositional systems in Lake Corinth in the central rift were strongly affected by intrabasin faults. Palaeocurrents suggest flow paths changing from northerly (transverse) to easterly (axial), recording sub-lacustrine turbidity currents flowing in channel belts parallel to, and located in the immediate hanging wall of, active normal faults (Fig. 13a). Comparison with the western part of the present-day Gulf of Corinth is apt, as is the provenance data for the Pellini Formation turbidites, which suggests sediment sourced from a N-flowing palaeo-Olvios river, via the Kyllini delta, or from the Kalavryta drainage further west between *ca.* 3.6 and 3.3 Ma. Metamorphic clasts within the Rethi-Dendro Formation turbidites, suggest a genetic link to the Mavro delta and exhumation and erosion of the Phyllites-Quartzites nappe in the catchment of the palaeo-Olvios river between 3.3 and 1.8 Ma (Fig. 13a). Although data from the rift axis further east is currently limited, we suspect a similar scenario existed for the Stymfalia and Nemea catchments, both supplying turbidites that were ‘ponded’ in fault-controlled depocentres along the rift axis (Fig. 13a).

In contrast with the deepening upward trend and deep lacustrine conditions that dominated much of Rift 1 in the main rift depocentre, the Megara basin to the east was characterized by an overall shallowing-upward trend from sub-lacustrine to northerly flowing axial fluvial deposits (Bentham *et al.*, 1991) (Figs 12 and 13a). Clasts within the deltaic to fluvial infill of the basin are dominated serpentinite and chert derived from ophiolites in the Pelagonian basement unit exposed on the Perachora-Geraneia horst (Bentham *et al.*, 1991) (Fig. 13a). Sediment sourced from the footwall of the Pateras fault to the NE has a limestone provenance and comprises only a minor proportion of the basin fill exposed today. High sediment supply from the relatively easily erodible ophiolitic units on the Perachora-Geraneia horst outpaced subsidence along the SW hanging wall dipslope of the Megara basin, leading to overfilled conditions and establishment of the axial fluvial system. This fluvial system extended to the NW, under the present-day Alkyonides gulf where it is now down-faulted by the younger, Rift 2, East and West Alkyonides faults (Leeder *et al.*, 2002, 2008) (cf. Fig. 13a, b). The Megara basin infill under the Alkyonides gulf would equate to offshore Seismic Unit 1 (Nixon *et al.*, 2016) and probably extends into the Gilbert reverse chron, (>3.58 Ma), based on palaeomagnetic data tied to dated ash within the onshore part of the Megara basin (Leeder *et al.*, 2008).

Brackish incursions within the Harbour Ridges Formation (Bentham *et al.*, 1991) suggest the Megara basin was not entirely closed, but underwent occasional marine incursions from the NW (Fig. 13a). Episodic marine influence is also recorded in the deep-water lacustrine turbidites and hemipelagic marls of the Aiges Formation (Rethi-Dendro Formation equivalent) in the western part of the rift (Rohais *et al.*, 2007a). Our palaeogeographic reconstruction suggests that this marine connection had to be from the proto-Saronic Gulf through the Corinth basin, as Rift 1 was closed to the west (Fig. 13a).

Rift 2 from 2.2–1.8 Ma to present

In this phase, a 15–30 km northward shift in fault activity forced the locus of rifting to its current location under the Gulf of Corinth, with Rift 2 initially focused on a 20–30 km-wide zone, bounded by N- and S-dipping faults (Bell *et al.*, 2009; Nixon *et al.*, 2016) (Fig. 13b). All the southern border faults and fault blocks that were active during Rift 1 in the west and central part of rift died, as did the faults bounding the Megara basin (Fig. 13b). The onset of Rift 2 is constrained by a combination of magnetostratigraphy and radiometric dating of the Pagae ash in the eastern rift (Megara basin) to *ca.* 2.2 Ma (Leeder *et al.*, 2008) and by palynology in the west-central part of the rift to *ca.* 1.8 Ma (Malartre *et al.*, 2004; Rohais *et al.*, 2007a,b; Ford *et al.*, 2013). Although there is uncertainty in these constraints, they suggest that the change in fault activity may have been diachronous along the length of the rift, beginning earlier in the east, as with the development of Rift 1 (Fig. 12).

The timing of fault activity and evolution during Rift 2 is better constrained than for Rift 1 by onshore and offshore studies, particularly for the last *ca.* 0.6 Myr (Nixon *et al.*, 2016). We view minor northward and southward shifts in active faulting, and changes in fault polarity and rift symmetry during Rift 2 as being associated with organization of the fault network to produce an asymmetric rift with a dominant, linked border fault (cf. Cowie, 1998; Cowie *et al.*, 2000; Nixon *et al.*, 2016). In the westernmost part of the rift pronounced northward and westward migration of activity is interpreted as due to interaction of the Corinth rift with the Patras rift (Figs 12 and 13b, c).

In the western and central parts of the rift, Rift 2 deformation was initially associated with both N- and S-dipping faults and the rift has a symmetrical, graben-like geometry, 15–25 km wide (Bell *et al.*, 2009; Taylor *et al.*, 2011; Nixon *et al.*, 2016). Along the southern rift margin a series of 10–20 km long, N-dipping fault segments (e.g. Lakka, Panachaikon, Pyrgaki, Mamoussia and Valimi faults) accumulated 1–3 km of throw. The northern margin of the rift is defined by S-dipping faults with up to 1.3 km of throw (e.g. Trizonia, West Channel and Galaxidi faults) (Fig. 13b). Northward migration of fault activity occurred at *ca.* 0.8 Ma, with death of the Pyrgaki, Mamoussia and Valimi faults and initiation of the East and West Heliki faults (Fig. 12 and cf. Fig. 13b, c). Activity on the S-dipping faults decreased between 0.6 and 0.3 Ma with many becoming inactive by 0.4 Ma leading to an asymmetric rift with a dominant, N-dipping southern border fault (Bell *et al.*, 2008, 2009; Nixon *et al.*, 2016). The main exceptions are the North and South Eratini faults, which became active after 0.6 Ma (McNeill *et al.*, 2005; Bell *et al.*, 2009). In the westernmost part of the rift, around the Trizonia fault, northward migration of activity on both northern and southern margins of the rift has occurred in the last 0.4 Ma, with activity migrating onto the Psathopyrgos fault and Neos Erineos fault system along the southern margin, and from the Trizonia fault onto the Marathias and Nafpakos faults along the northern margin (Beckers *et al.*, 2015) (Fig. 13c).

The central part of the rift has developed an essentially half-graben geometry, with N-dipping faults along the southern margin becoming dominant during Rift 2. The West Xylokastro fault was certainly active at 1.0 Ma (Fig. 13b), based on dating of syntectonic calcite cements from the fault zone (Flotte *et al.*, 2001; Causse *et al.*, 2004), and probably continued to be active until 0.8–0.6 Ma, based on uplift rates and terminal topset elevations of uplifted coarse-grained deltas. Fault activity then shifted northward onto the Derveni fault, linking eastwards with the Lykoporia fault by *ca.* 0.4–0.3 Ma (Nixon *et al.*, 2016) (cf. Fig. 13b, c). Linkage and localization of strain onto the dominant southern border fault continued with breaching of the relay between the Derveni and East Heliki faults between 0.4–0.3 Ma (Hemelsdaël & Ford, 2016). Associated with this strain localization, many of the S-dipping faults under the central Gulf of Corinth died (e.g. Antikyra faults) and became buried (Nixon *et al.*, 2016) (Fig. 13c).

In the eastern rift, the Perachora-Geraneia horst remained a major structural high during Rift 2. Its westward offshore continuation, the Heraion ridge, separates the main Corinth rift from the Lechion gulf and Corinth basin (Fig. 13b). To the north of the horst, the N-dipping Perachora, Strava and West and East Alkyonides and Psatha faults became active together, bounding the Alkyonides gulf to the north, with several closely spaced faults on the Perachora Peninsula, including the Skinos and Pisa faults (Jackson *et al.*, 1982; Leeder *et al.*, 1991; Sakellariou *et al.*, 2007; Roberts *et al.*, 2009; Duffy *et al.*, 2015; Nixon *et al.*, 2016) (Fig. 13b). In contrast, major faults bounding the Corinth basin were largely inactive during Rift 2 times, although intrabasin faulting continued, creating local depocentres and highs (Collier, 1990; Collier & Dart, 1991).

The northward shift at the onset of Rift 2 had a major impact on depositional environments, stratigraphic evolution and the drainage systems (Fig. 12). The geomorphology inherited from Rift 1 has played a significant role in controlling the along-strike variability in depositional systems and stratigraphic evolution. In the far west of the rift a major new fluvial system (Rodini system), sourced from erosion of the Pindos thrust sheet to the north, prograded in a southerly direction across the rift and passed laterally into lacustrine deposits containing evidence of marine incursions (Palyvos *et al.*, 2008, 2010; Ford *et al.*, 2016) (Figs 12 and 13b). Shift of activity onto the Psathopyrgos and Marathias faults at around 0.4 Ma (Beckers *et al.*, 2015; Ford *et al.*, 2016), led to flooding and northward retreat of the Rodini delta system and opening of a marine connection to the Ionian Sea to the west via the Patras rift (Figs 12 and 13c). Uplift of the footwall of the Psathopyrgos fault caused offlap and downstep of highstand marine terraces between it and the Panachaikon-Lakka faults from at least MIS 11 (Palyvos *et al.*, 2008, 2010).

In the west-central part of the rift, major Gilbert-type coarse-gained delta complexes along the immediate hanging wall of the growing southern border fault mark the start of Rift 2 deposition (Figs 12 and 13b). Valley-like erosional truncation of Rift 1 stratigraphy underlies some of these deltas, e.g. the Vouraikos delta (Backert *et al.*, 2010; Ford *et al.*, 2013), suggesting that development of a juvenile stream network had already taken place prior to surface rupture of the new southern border fault. Stream networks eroded headwards, driven by footwall uplift, to capture parts of the Rift 1 Kalavryta drainage system, creating major S- to N-flowing rivers, spaced 6–8 km along the newly established range front. Some of these locally exploited relay ramps between fault segments (e.g. Kerinitis) (Fig. 13b). Basinward of the deltas, turbidite and hemipelagic deposits are likely to form the main facies in offshore Seismic Unit 1 (Nixon *et al.*, 2016), with local structural control on sediment transport pathways and fan deposition (Fig. 13b).

Death of the Pyrgaki, Mamoussia and Valimi faults and northward shift in fault activity to the West and East Helike faults and the Derveni fault caused abandonment and uplift of these coarse-grained delta complexes, starting around 0.8 Ma (Rohais *et al.*, 2007b; Ford *et al.*, 2013) (Figs 12 and 13c). Rivers maintained their flow direction, incising the now-abandoned deltas and the prerift units in the newly uplifting footwall, and supplied sediment to form new delta complexes at their mouths along the Helike range front (Fig. 13c). At the eastern end of the East Heliki fault, drainage was focused through the relay ramp between it and the Derveni fault (Hemelsdaël & Ford, 2016). Basinward of these deltas major submarine channels and canyons developed, creating a subaqueous sediment dispersal system similar to that of today (McNeill *et al.*, 2005).

In the central part of the rift, the West Xylokastro fault grew within a lacustrine basin inherited from Rift 1, but close to the major Olvios river. The Rift 1 Mavro delta was abandoned and incised by this river, which continued to flow northwards, focused though the segment boundary between the Valimi and West Xylokastro faults, to feed the Evrostini and Ilias deltas (Fig. 13b). These deltas prograded into deep water, as indicated by the *ca.* 500 m high foresets of the Evrostini delta (Ori, 1989; Rohais *et al.*, 2007a, 2008), and growth faulting is evident in the Evrostini delta in what was a zone of high sediment supply and deposition (Rohais *et al.*, 2007a). Basinward of these deltas, the turbidite channel and lobe complexes of the Rethi-Dendro and Aiges formations developed, with flows captured by fault-controlled hanging wall subsidence to run axially, for example in the hanging wall of the West Xylokastro fault (Fig. 13b). Subsequent death of this structure at around 0.8 Ma and localization of slip onto the Derveni-Lykoporia faults to the north uplifted the Xylokastro fault block and horst (Fig. 13c).

Further east, the southern shoreline and coarse-grained deltas are located over 20 km to the south of the developing Rift 2 southern border fault (Lykoporia, East Xylokastro, North Kiato faults) (cf. Fig. 13a and b). As a consequence their hanging walls are sediment starved, as indicated by the dominance of the Rethi-Dendro Formation in the hanging wall of the eastern part of the West Xylokastro fault, and by relative thins on time-thickness maps of Seismic Unit 1 in the hanging wall of the Lykoporia and East Xylokastro faults (Nixon *et al.*, 2016). The stratal geometry and stratigraphy of the deltas in this area are significantly different from the giant Gilbert-type deltas further west. A good example is the Kryoneri delta, sourced from the N-flowing Stymfalia river. Here, the downstepping, erosionally based, progradational delta terraces form an overall forced-regressive package, interpreted to record the uplift, progressive shallowing and destruction of Lake Corinth inherited from Rift 1 times (Fig. 13b). Initially the main Olvios, Stymfalia and Nemea rivers maintained a northward course, but they were eventually reversed, reducing sediment supply to depocentres in the central and eastern parts of the rift, although new juvenile drainage eroded headwards into relatively poorly consolidated syn-rift sediments (Seger & Alexander, 1993; Gawthorpe *et al.*, 1994; Zelilidis, 2000), (cf. Fig. 13b, c). Reversal of the Stymfalia system is recorded by the end of deposition of the Kryoneri delta and a change to wave-dominated shoreline facies capping younger, lower elevation terraces. In parts of the eastern rift, low clastic sediment supply, resulting from drainage diversion or reversal, promoted local development of carbonate facies during marine transgressions and highstands including both coral and red algal and microbial buildups (Portman *et al.*, 2005), carbonate shoals (Collier & Thompson, 1991), and rocky shoreline facies (Palyvos *et al.*, 2008).

Reversal of drainage also occurred in the east of the rift, where initiation and growth of the East and West

Alkyonides and Psatha faults around 2.2 Ma caused uplift and back-tilting of the Megara basin (Fig. 13b). Headward erosion from these faults and the Pisia and Skinos faults to the west caused development of new N-flowing footwall-sourced drainage supplying sediment to small shoreline fan deltas and locally bypassing sediment to the basin floor (Leeder *et al.*, 1991, 2002). At the very eastern end of the Corinth rift, propagation of the Psatha fault into the Pateras Range caused beheading of drainage, development of wind gaps and creation of small internally drained basins (Morewood & Roberts, 2002) (Fig. 13c).

A major change in the offshore Rift 2 stratigraphy is recorded across almost the entire rift between Seismic Unit 1 and Seismic Unit 2 (Nixon *et al.*, 2016). It marks the change, estimated to occur at *ca*. 0.6 Ma, from Lake Corinth, with intermittent marine incursions, to a periodically fully marine Gulf of Corinth connected to open ocean during interglacial highstands (Nixon *et al.*, 2016). We infer that this 'Great Breaching' must have been due to structural/erosional elimination of land barriers at the eastern (Corinth Isthmus) and/or western (Rion Straits) limits to the rift. Regional uplift combined with intrabasinal faulting on the Corinth Isthmus created complex topography affecting deposition and eventually entirely closed the connection to the wholly marine Saronic Gulf around 0.1 Ma.

Although the distinctive high/low amplitude seismic reflectance layering of Seismic Unit 2 has been interpreted to reflect 100 kyr glacio-eustatic cyclicity (see review by Nixon *et al.*, 2016), there is currently no clear sedimentological model to explain the alternations in seismic facies. We know that during glacial lowstands Lake Corinth was characterized by high sediment-yield winter runoff (Collier *et al.*, 2000). This would have caused frequent hyperpycnal underflows that ventilated the rift bottom waters. By contrast, highstand marine interludes had lower sediment yields, due to more forest cover and less runoff so that the saline ambient gulf waters would have encouraged hypopycnal conditions that caused wide dispersal of surface plumes and possible anoxia in poorly ventilated bottom waters. We await results from deep coring of the offshore stratigraphy by IODP Expedition 381 to test this suggestion.

IMPLICATIONS FOR TECTONO-SEDIMENTARY DEVELOPMENT OF RIFT BASINS

In the following discussion we focus on aspects of the tectono-stratigraphic evolution of the Corinth rift that can be applied to rift basins globally. We highlight three specific themes of particular importance for rift tectono-stratigraphic models: (i) fault network organization and rift migration, (ii) the role of inherited topography and antecedent drainage, and (iii) syn-rift stratigraphic evolution and sequence stratigraphic variability.

Fault network organization and rift migration

Recent studies of the offshore Corinth rift have highlighted the detailed geometry and evolution of the offshore fault array (e.g. Bell *et al.*, 2009; Taylor *et al.*, 2011; Nixon *et al.*, 2016). The development of the fault network displays similar evolutionary characteristics during both phases – Rift 1 and Rift 2: (i) initiation and growth of a distributed conjugate fault network, (ii) segment growth and linkage, (iii) early development of dip domains, (iv) minor shifts in fault activity with new faults developing and some faults dying, associated with, (v) progressive evolution of rift asymmetry with development of a border fault system, and (vi) rapid linkage and localization of deformation onto the border fault system (Bell *et al.*, 2009; Nixon *et al.*, 2016; this study). This style of structural evolution is characteristic of many rifts, including the Gulf of Suez, East African rift and northern North Sea (e.g. Ebinger *et al.*, 1999; Gawthorpe *et al.*, 2003; Cowie *et al.*, 2005), and can be largely explained by self-organization of the fault network (Cowie, 1998; Cowie *et al.*, 2000, 2005). The dramatic migration in rift location between Rift 1 and Rift 2 cannot, however, be readily explained by self-organization of the Rift 1 normal fault network. New insights await models of strain localization in the upper plate above subducting slabs.

Role of inherited topography and antecedent drainage

The role of pre-existing (inherited) topography and drainage on the geomorphology and tectono-sedimentology of rifts is not clearly addressed in many studies of rift basins, although antecedent drainage is incorporated into some conceptual models (e.g. Gawthorpe & Leeder, 2000). Forward models of rift development incorporating surface processes mainly start with a flat upper surface, such that the landscape and drainage system derives uniquely from the tectonic and climatic activity during rifting (e.g. Cowie *et al.*, 2006). Furthermore, studies investigating climate and tectonic controls on erosion and syn-rift stratigraphy tend to focus on single footwall catchment-hanging wall fan systems (e.g. Armitage *et al.*, 2011).

The Corinth rift developed across an area with significant palaeorelief inherited from the Hellenide mountain belt. On a regional scale, relatively high topography occurs both north and south of the rift in the west compared to the east (Fig. 1). The strike of this topography parallels the strike of Hellenide folds and thrusts and we interpret this regional (hundred kilometre) E-W topographic gradient to be at least partly inherited from the Hellenide mountain belt. This pre-rift topographic template exerted a first-order control on the position of regional sea- or lake-level and regional slope gradients (sediment transport pathways), and therefore on gross depositional environments during rifting. Rift 1, for example, is partitioned into largely fluvial deposition in the west and lacustrine deposition further east, with dominantly eastward-flowing axial depositional systems (Fig. 13a).

Superimposed on this regional topography there is marked local valley-like topographic relief of several hundred metres that is partly filled by early syn-rift fluvial conglomerates. The scale of this erosional topography and the early syn-rift fluvial deposits within the palaeovalleys suggest that it is related to antecedent rivers draining the Hellenide mountain belt (e.g. Fig. 13a), rather than simply local consequent drainage developed in the footwall of newly active normal faults. Four main antecedent catchments, spaced approximately 20 km apart and extending several tens of kilometres into the southern rift flank, supplied the majority of sediment to the Corinth rift (Fig. 13a). These catchments are over an order of magnitude larger than consequent footwall catchments developed along normal fault zones, for example catchments along the active Skinos and Pisia Faults in the eastern part of the rift (Leeder *et al.*, 1991, 2002). They were also long-lived sediment sources throughout most of the evolution of the rift and, although they locally exploited relay zones between fault segments, their stream power was high enough to maintain their course by eroding through uplifting basement-cored footwall blocks.

Although not clearly documented from many rifts, the role of inherited, pre-rift topography is signalled as important in the East African rift. For example, the Malawi rift cuts across a dominantly west to east drainage system (e.g. Ruvuma catchment) such that catchments draining into the rift are asymmetric, with larger catchments on the west side than the east (Crossley, 1984). Furthermore, in a similar way to the Corinth rift, the location of many of the main rivers entering the Malawi rift is interpreted to be controlled by pre-rift topography (Crossley, 1984). In contrast, in the late Jurassic axis rift of the northern North Sea pre-rift topography was subtle, with the Brent delta developed across much of the area and forming a low gradient delta plain prior to rifting. During the initial stages of rifting, the easily erodible pre-rift sediments and continuing high sediment supply from the Brent delta helped to maintain relatively flat depositional topography, but nevertheless with subtle hanging wall depocentres that were occupied by estuaries and focused sedimentation (e.g. channel belts) and tidal currents (Løseth *et al.*, 2009).

The Corinth rift and the examples from the East African rift system and the northern North Sea illustrate the important, but variable, impact pre-rift geomorphology has on sediment source areas, sediment transport pathways and gross depositional environments during rifting. Pre-rift tectonics, the latest pre-rift drainage and sedimentary systems, and bedrock lithology all play a role in developing the topographic template that the rift inherits, but how this influences syn-rift tectono-stratigraphy is also a function of the orientation of the rift relative to the pre-existing structure and drainage.

Syn-rift stratigraphic evolution and sequence stratigraphic variability

Syn-rift stratigraphic evolution

We have already discussed the importance of antecedent drainage in controlling the location and volume of sediment supplied into rifts compared to consequent footwall scarp drainage. High sediment supply from large antecedent catchments can potentially overwhelm hanging wall subsidence, particularly during the early stages of rifting when extension is distributed across a number of developing normal faults and displacement rates are low.

This is highlighted by the Rift 1 fluvial systems sourced from the Kalavryta drainage in the west of the rift, which is highly progradational and overfilled several developing fault blocks (Hemelsdaël *et al.*, 2017) (Fig. 13a). In this depositional system, downstream gradient and grain size variations were largely unaffected by the local fault-controlled subsidence and uplift; rather they were primarily controlled by the high sediment and water flux from the antecedent catchments (Hemelsdaël *et al.*, 2017). High sediment supply can also be derived from areas where bedrock lithologies are easily erodible, for example the serpentinized ophiolitic units of the pre-rift on the Perachora-Geraneia horst. Here, the syn-rift deposits within the adjacent Megara basin display an overall shallowing upward, progradational motif, consistent with sediment supply outpacing local subsidence (Fig. 13a).

In contrast, the central part of Rift 1 becomes largely sediment starved and the site of Lake Corinth (Fig. 9). Here, the succession deepens upward from fluvial to deep lacustrine and the depositional systems are highly influenced by local faulting. For example, in the Rethi-Dendro Formation, deep lacustrine turbidite channels are funnelled axially, eastward along the hanging walls of active normal faults (e.g. Fig. 13a). With the exception of the western part of the rift, Rift 2 was also sediment starved and underfilled throughout its evolution (Fig. 13b, c). This may in part be function of higher extension rates (Ford *et al.*, 2013), but the fact that several of the main antecedent sediment input points to the central part of the rift became located 10–30 km south of the Rift 2 southern border fault meant that sediment supply to the rift axis was significantly reduced.

Models for the large-scale evolution of rift basin stratigraphy tend to stress an evolution from overfill or balanced fill during the early stages of rifting to underfilled during the later stages (e.g. Leeder & Gawthorpe, 1987; Prosser, 1993; Ravnas & Steel, 1998; Gawthorpe & Leeder, 2000). Although this motif may be common in rift axis locations, the stratigraphy along the Corinth rift suggests a much more variable stratigraphic motif may be typical along the margin of the rift, particularly where large antecedent catchments enter the rift, as in the example of the Kalavryta system in the western Corinth rift. In these locations sediment supply may be able to keep pace or overfill fault-controlled subsidence leading to shallowing-upward stratigraphic motifs.

Sequence stratigraphic variability

At higher stratigraphic resolution, key stratal surfaces, such as flooding surfaces and exposure/incision surfaces, and facies stacking patterns in rift basins are predicted to have limited spatial extent because of variations in fault-controlled subsidence and uplift, and changes in sediment supply (e.g. Gawthorpe *et al.*, 1994). A clear example of this is provided by the succession developed along the southern shoreline of the rift during Rift 2 times. In the west, the shoreline is located in the hanging wall of the developing southern border fault, where thick aggradationally stacked fan deltas occur compose of a series of aggradational to progradational stratal units bounded by flooding surfaces (e.g. Dart *et al.*, 1994; Backert *et al.*, 2010). Examples in the Corinth rift include the Kerinitis and Vouraikos deltas in the hanging wall of the Pyrgaki and Mamoussia faults; Fig. 13b). In contrast, in the central rift, the shoreline was located in the footwall of the newly developing southern border fault and thus subject to uplift. In this area the stratigraphy of the Kryoneri delta (Fig. 13b) is markedly different, and comprises an overall downstepping and offlapping pattern where the older parts of the delta are progressively incised by their own drainage, all characteristics of forced regression and relative sea-level fall.

The evolution of the Kryoneri delta also highlights the importance of changes in sediment supply on depositional environment and facies in rift margin settings. Death of the Kryoneri delta resulted from reversal of the Stymfalia drainage, which produced a major facies change in the younger shoreline deposits to wave-dominated shoreface facies associations. Drainage reversal and the associated facies changes do not appear to have been related to specific changes in tectonics or climate; rather they are the result of the progressive evolution and organization of the drainage network supplying sediment to the rift.

The along-strike variations in sedimentology and stratigraphy highlight the problems that arise in correlation at both the fault segment and rift scale. Such complexity helps to explain some of the contradictory interpretations of tectono-stratigraphic evolution of the Corinth rift (e.g. Rohais *et al.*, 2007a; Leeder *et al.*, 2012; Ford *et al.*, 2013, 2016), as well as other rifts such as the northern North Sea (Ravnas & Steel, 1998). We suggest a pragmatic approach to the tectono-sedimentary analysis of rifts that involves: (a) establishing a robust chronostratigraphic framework, (b) identification and mapping of tectonically enhanced major flooding surfaces, and (c) integration of sedimentological and structural analysis. Major developments in the Corinth rift will revolve around advances in the chronostratigraphic framework.

CONCLUSIONS

The central onshore geology of the Corinth rift contains a syn-rift succession >3 km thick deposited in 5–15 km-wide tilt blocks. The succession deepens upward from fluvial to deep lacustrine, establishing a lake, Lake Corinth, over most of the rift by 3.6 Ma. From *ca.* 1.8 Ma the succession was progressively uplifted, unconformably overlain by deltaic and shallow marine deposits, and eroded.

The rift developed in two main phases. Rift 1, from 5.0–3.6 to 2.2–1.8 Ma, was largely located onshore along the northern Peloponnesus and the Corinth and Megara basins. Rift 2, from 2.2–1.8 Ma to present, is focused on the present-day Gulf of Corinth. The switch from Rift 1 to Rift 2 is marked by a 30 km northward shift in the locus of rifting. Each rift phase displays a similar structural evolution from a distributed conjugate fault network to progressive development of rift asymmetry and the development of a dominant, linked border fault system along the southern rift margin.

Regional palaeotopography and antecedent drainage, inherited from the Hellenide mountain belt, exerted a major control on gross depositional environments, shoreline position, and the main sediment sources and syn-rift transport pathways. Sediment supply to the rift was asymmetric with four main N- to NE-flowing antecedent drainages along the southern rift flank major sources of sediment during both rift phases. One major S-flowing drainage in the west of the rift was active during Rift 2.

Syn-rift stratigraphic motifs show marked variation along the rift. Rift axis locations display an overall deepening upward trend, with rift structure strongly influencing sedimentary transport and deposition. Along the rift margin, however, strongly progradational, shallowing upward motifs are also developed in areas of high sediment supply. Facies stacking patterns and key sequence stratigraphic surfaces show marked variations over distances of tens of kilometres, particularly where the shoreline position changes from hanging wall to footwall.

The tectono-stratigraphic evolution of the relatively young (<5 Ma) Corinth rift highlights the complexity of rift evolution, the variability in rift basin sedimentology and stratigraphy, and the factors that combine to control the tectono-sedimentary development of rift basins. Our rift-wide study highlights the importance of pre-rift geology and geomorphology for rift evolution, and the need for a robust chronostratigraphic framework.

ACKNOWLEDGEMENTS

Part of the research within this paper was the Syn-Rift Systems project funded by Research Council of Norway (Project number 255229/E30) and industry partners Aker BP, ConocoPhillips, Faroe Petroleum, Statoil, Tullow Oil and VNG Norge for which we are grateful. The authors' thank the Segas family for help and support whilst undertaking fieldwork in the Corinth rift. Rebecca Bell, Richard Collier, Mary Ford and Casey Nixon are thanked for discussions on the Corinth rift. This paper was written when RLG was on sabbatical and he acknowledges the help and support provided by Lesli Wood and staff at the Department of Geology and Geological Engineering at Colorado School of Mines. Reviews by Lisa McNeill, Michael Hopkins and Liz Hajek and editorial steer from Cindy Ebinger are gratefully acknowledged. The authors have no conflict of interest to declare.

REFERENCES

Alonso-Zara, A.M. & Wright, V.P. (2010) Palustrine carbonates. In: *Carbonates in Continental Settings: Facies. Environments and Processes* (Ed. by A.M. Alonso-Zara, L.H. Tanner), pp. 103–131. Elsevier, Amsterdam.

Armijo, R., Meyer, B., King, G.C.P., Rigo, A. & Papanastassiou, D. (1996) Quaternary evolution of the Corinth Rift and its implications for the Late Cenozoic evolution of the Aegean. *Geophys. J. Int.*, **126**, 11–53.

Armitage, J.J., Duller, R.A., Whittaker, A.C. & Allen, P.A. (2011) Transformation of tectonic and climatic signals from source to sedimentary archive. *Nat. Geosci.*, **4**, 231–235.

Avallone, A., Briole, P., Agatza-Balodimou, A.M., Billiris, H., Charade, O., Mitsakaki, C., Nercessian, A., Papazissi, K., Paradissis, D. & Veis, G. (2004) Analysis of eleven years of deformation measured by GPS in the Corinth Rift Laboratory area. *C.R. Geosci.*, **336**, 301–311.

Backert, N., Ford, M. & Malartre, F. (2010) Architecture and sedimentology of the Kerinitis Gilbert-type fan delta, Corinth Rift, Greece. *Sedimentology*, **57**, 543–586.

Beckers, A., Hubert-Ferrari, A., Beck, C., Bodeux, S., Tripsanas, E., Sakellariou, D. & De Batist, M. (2015) Active faulting at the western tip of the Gulf of Corinth, Greece, from high-resolution seismic data. *Mar. Geol.*, **360**, 55–69.

Bell, R.E., McNeill, L.C., Bull, J.M. & Henstock, T.J. (2008) Evolution of the offshore western Gulf of Corinth. *Geol. Soc. Am. Bull.*, **120**, 156–178.

Bell, R.E., McNeill, L.C., Bull, J.M., Henstock, T.J., Collier, R.E.L. & Leeder, M.R. (2009) Fault architecture, basin structure and evolution of the Gulf of Corinth Rift, central Greece. *Basin Res.*, **21**, 824–855.

Bell, R.E., McNeill, L.C., Henstock, T.J. & Bull, J.M. (2011) Comparing extension on multiple time and depth scales in the Corinth Rift, Central Greece. *Geophys. J. Int.*, **186**, 463–470.

Bentham, P., Collier, R.E., Gawthorpe, R.L., Leeder, R. & Stark, C. (1991) Tectono-sedimentary development of an extensional basin: the Neogene Megara Basin, Greece. *J. Geol. Soc.*, **148**, 923–934.

Bernard, P., Lyon-Caen, H., Briole, P., Deschamps, A., Boudin, F., Makropoulos, K., Papadimitriou, P., Lemeille, F., Patau, G., Billiris, H., Paradissis, D., Papazissi, P., Castarede, H., Charade, O., Nercessian, A., Avallone, D., Pachiani, F., Zahradnik, J., Sacks, S. & Linde, A. (2006) Seismicity, deformation and seismic hazard in the western rift of Corinth: New insights from the Corinth Rift Laboratory (CRL). *Tectonophysics*, **426**, 7–30.

Bouma, A.H. (1962) *Sedimentology of Some Flysch Deposits; a Graphic Approach to Facies Interpretation*, p. 167. Elsevier, Amsterdam.

Brasier, A.T., Andrews, J.E., Marca-Bell, A.D. & Dennis, P.F. (2010) Depositional continuity of seasonally laminated tufas: implications for delta O-18 based palaeotemperatures. *Global Planet. Change*, **71**, 160–167.

Brasier, A.T., Andrews, J.E. & Kendall, A.C. (2011) Diagenesis or dire genesis? The origin of columnar spar in tufa stromatolites of central Greece and the role of chironomid larvae. *Sedimentology*, **58**, 1283–1302.

Bridge, J.S. (1993) Description and interpretation of fluvial deposits – a critical perspective. *Sedimentology*, **40**, 801–810.

Bridge, J.S. (2003) *Rivers and Floodplains: Forms, Processes, and the Sedimentary Record*. Blackwell Science Ltd, Oxford.

Briole, P., Rigo, A., Lyon-Caen, H., Ruegg, J.C., Papazissi, K., Mitsakaki, C., Balodimou, A., Veis, G., Hatzfeld, D. & Deschamps, A. (2000) Active deformation of the Corinth rift, Greece: results from repeated Global Positioning System surveys between 1990 and 1995. *J. Geophys. Res.-Solid Earth*, **105**, 25605–25625.

Causse, C., Moretti, I., Eschard, R., Micarelli, L., Ghaleb, B. & Frank, N. (2004) Kinematics of the Corinth Gulf inferred from calcite dating and syntectonic sedimentary characteristics. *C.R. Geosci.*, **336**, 281–290.

Charalampakis, M., Lykousis, V., Sakellariou, D., Papatheodorou, G. & Ferentinos, G. (2014) The tectono-sedimentary evolution of the Lechaion Gulf, the south eastern branch of the Corinth graben, Greece. *Mar. Geol.*, **351**, 58–75.

Clarke, P.J., Davies, R.R., England, P.C., Parsons, B.E., Billiris, H., Paradissis, D., Veis, G., Denys, P.H., Cross, P.A., Ashkenazi, V. & Bingley, R. (1997) Geodetic estimate of seismic hazard in the Gulf of Korinthos. *Geophys. Res. Lett.*, **24**, 1303–1306.

Clarke, P.J., Davies, R.R., England, P.C., Parsons, B., Billiris, H., Paradissis, D., Veis, G., Cross, P.A., Denys, P., Ashkenazi, V., Bingley, R., Kahle, H.-G., Muller, M.V. & Briole, P. (1998) Crustal strain in central Greece from repeated GPS measurements in the interval 1989-1997. *Geophys. J. Int.*, **135**, 195–214.

Collier, R.E.L. (1990) Eustatic and tectonic controls upon quaternary coastal sedimentation in the Corinth Basin, Greece. *J. Geol. Soc.*, **147**, 301–314.

Collier, R.E.L. & Dart, C.J. (1991) Neogene to quaternary rifting, sedimentation and uplift in the Corinth Basin, Greece. *J. Geol. Soc.*, **148**, 1049–1065.

Collier, R.E.L.L. & Thompson, J. (1991) Transverse and Linear Dunes in an Upper Pleistocene Marine Sequence, Corinth Basin, Greece. *Sedimentology*, **38**, 1021–1040.

Collier, R.E.L., Leeder, M.R., Trout, M., Ferentinos, G., Lyberis, E. & Papatheodorou, G. (2000) High sediment yields and cool, wet winters: test of last glacial paleoclimates in the northern Mediterranean. *Geology*, **28**, 999–1002.

Cowie, P.A. (1998) A healing-reloading feedback control on the growth rate of seismogenic faults. *J. Struct. Geol.*, **20**, 1075–1087.

Cowie, P.A., Gupta, S. & Dawers, N.H. (2000) Implications of fault array evolution for synrift depocentre development: insights from a numerical fault growth model. *Basin Res.*, **12**, 241–261.

Cowie, P.A., Underhill, J.R., Behn, M.D., Lin, J. & Gill, C.E. (2005) Spatio-temporal evolution of strain accumulation derived from multi-scale observations of Late Jurassic rifting in the northern North Sea: a critical test of models for lithospheric extension. *Earth Planet. Sci. Lett.*, **234**, 401–419.

Cowie, P.A., Attal, M., Tucker, G.E., Whittaker, A.C., Naylor, M., Ganas, A. & Roberts, G.P. (2006) Investigating the surface process response to fault interaction and linkage using a numerical modelling approach. *Basin Res.*, **18**, 231–266.

Crossley, R. (1984) Controls of sedimentation in the Malawi Rift Valley, Central Africa. *Sed. Geol.*, **40**, 33–50.

Dart, C.J., Collier, R.E.L., Gawthorpe, R.L., Keller, J.V.A. & Nichols, G. (1994) Sequence stratigraphy of ()Pliocene-quaternary synrift, gilbert-type fan deltas, Northern Peloponnesos, Greece. *Mar. Pet. Geol.*, **11**, 545–560.

Davies, R., England, P., Parsons, B., Billiris, H., Paradissis, D. & Veis, G. (1997) Geodetic strain of Greece in the interval 1892–1992. *J. Geophys. Res.-Solid Earth*, **102**, 24571–24588.

Doutsos, T. & Piper, D.J.W. (1990) Listric faulting, sedimentation, and morphological evolution of the quaternary Eastern Corinth Rift, Greece – 1st stages of continental rifting. *Geol. Soc. Am. Bull.*, **102**, 812–829.

Duffy, O.B., Brocklehurst, S.H., Gawthorpe, R.L., Leeder, M.R. & Finch, E. (2015) Controls on landscape and drainage evolution in regions of distributed normal faulting: Perachora Peninsula, Corinth Rift, Central Greece. *Basin Res.*, **27**, 473–494.

Ebinger, C.J., Jackson, J.A., Foster, A.N. & Hayward, N.J. (1999) Extensional basin geometry and the elastic lithosphere. *Philos. Transact. Royal Soc. Math. Phys. Eng. Sci.*, **357**, 741–762.

Flotte, N., Plagnes, V., Sorel, D. & Benedicto, A. (2001) Attempt to date Pleistocene normal faults of the Corinth-Patras Rift (Greece) by U/Th method, and tectonic implications. *Geophys. Res. Lett.*, **28**, 3769–3772.

Floyd, M.A., Billiris, H., Paradissis, D., Veis, G., Avallone, A., Briole, P., McClusky, S., Nocquet, J.M., Palamartchouk, K., Parsons, B. & England, P.C. (2010) A new velocity field for Greece: implications for the kinematics and dynamics of the Aegean. *J. Geophys. Res.-Solid Earth*, **115**, https://doi.org/10.1029/2009jb007040.

Ford, M., Rohais, S., Williams, E.A., Bourlange, S., Jousselin, D., Backert, N. & Malartre, F. (2013) Tectono-sedimentary evolution of the western Corinth rift (Central Greece). *Basin Res.*, **25**, 3–25.

Ford, M., Hemelsdael, R., Mancini, M. & Palyvos, N. (2016) Rift migration and lateral propagation: evolution of normal faults and sediment-routing systems of the western Corinth rift (Greece). In: *The Geometry of Normal Faults* (Ed. by Childs C., Holdsworth R.E., Jackson C.A-L., Manzocchi T., Walsh J.J., Yielding G.) Geol. Soc. London, Spec. Publ., (439) London.

Gawthorpe, R.L. & Leeder, M.R. (2000) Tectono-sedimentary evolution of active extensional basins. *Basin Res.*, **12**, 195–218.

Gawthorpe, R.L., Fraser, A.J. & Collier, R.E.L. (1994) Sequence stratigraphy in active extensional basins – implications for the interpretation of ancient basin-fills. *Mar. Pet. Geol.*, **11**, 642–658.

Gawthorpe, R.L., Sharp, I., Underhill, J.R. & Gupta, S. (1997) Linked sequence stratigraphic and structural evolution of propagating normal faults. *Geology*, **25**, 795–798.

Gawthorpe, R.L., Jackson, C.A.L., Young, M.J., Sharp, I.R., Moustafa, A.R. & Leppard, C.W. (2003) Normal fault growth, displacement localisation and the evolution of normal fault populations: the Hammam Faraun fault block, Suez rift, Egypt. *J. Struct. Geol.*, **25**, 883–895.

Gobo, K., Ghinassi, M. & Nemec, W. (2014) Reciprocal changes in foreset to bottomset facies in a gilbert-type delta: response to short-term changes in base level. *J. Sediment. Res.*, **84**, 1079–1095.

Gobo, K., Ghinassi, M. & Nemec, W. (2015) Gilbert-type deltas recording short-term base-level changes: delta-brink morphodynamics and related foreset facies. *Sedimentology*, **62**, 1923–1949.

Hemelsdaël, R. & Ford, M. (2016) Relay zone evolution: a history of repeated fault propagation and linkage, central Corinth rift, Greece. *Basin Res.*, **28**, 34–56.

Hemelsdaël, R., Ford, M., Malartre, F. & Gawthorpe, R.L. (2017) Interaction of an antecedent fluvial system with early normal fault growth: implications for syn-rift stratigraphy, western Corinth rift (Greece). *Sedimentology*, https://doi.org/10.1111/sed.12381.

Jackson, J.A., Gagnepain, J., Houseman, G., King, G.C.P., Papadimitriou, P., Soufleris, C. & Virieux, J. (1982) Seismicity, normal faulting, and the geomorphological development of the Gulf of Corinth (Greece) – the Corinth earthquakes of February and March 1981. *Earth Planet. Sci. Lett.*, **57**, 377–397.

Keraudren, B. & Sorel, D. (1987) The terraces of Corinth (Greece) – a detailed record of Eustatic sea-level variations during the last 500,000 years. *Mar. Geol.*, **77**, 99–107.

Koutsouveli, A., Mettos, A., Tsapralis, V., Tsaila-Monopoli, S. & Ioakim, C. (1989) *Geological map of Greece: 1:50,000, Xylokastro Sheet*. IGME Publications, Athens, Greece.

Leeder, M.R. & Gawthorpe, R.L. (1987) Sedimentary models for extensional tilt-block/half-graben basins. *Geol. Soc. London Spec. Publ.*, **28**, 139–152.

Leeder, M.R., Seger, M.J. & Stark, C.P. (1991) Sedimentation and tectonic geomorphology adjacent to major active and inactive normal faults, Southern Greece. *J. Geol. Soc.*, **148**, 331–343.

Leeder, M.R., Collier, R.E.L., Aziz, L.H.A., Trout, M., Ferentinos, G., Papatheodorou, G. & Lyberis, E. (2002) Tectono-sedimentary processes along an active marine/lacustrine half-graben margin: Alkyonides Gulf, E. Gulf of Corinth, Greece. *Basin Res.*, **14**, 25–41.

Leeder, M.R., Mack, G.H., Brasier, A.T., Parrish, R.R., McIntosh, W.C., Andrews, J.E. & Duermeijer, C.E. (2008) Late-Pliocene timing of Corinth (Greece) rift-margin fault migration. *Earth Planet. Sci. Lett.*, **274**, 132–141.

Leeder, M.R., Mark, D.F., Gawthorpe, R.L., Kranis, H., Loveless, S., Pedentchouk, N., Skourtsos, E., Turner, J., Andrews, J.E. & Stamatakis, M. (2012) A "Great Deepening": chronology of rift climax, Corinth rift, Greece. *Geology*, **40**, 999–1002.

Løseth, T.M., Ryseth, A.E. & Young, M. (2009) Sedimentology and sequence stratigraphy of the middle Jurassic Tarbert Formation, Oseberg South area (northern North Sea). *Basin Res.*, **21**, 597–619.

Lunt, I.A., Bridge, J.S. & Tye, R.S. (2004) A quantitative, three-dimensional depositional model of gravelly braided rivers. *Sedimentology*, **51**, 377–414.

Lykousis, V., Sakellariou, D., Moretti, I. & Kaberi, H. (2007) Late Quaternary basin evolution of the Gulf of Corinth: Sequence stratigraphy, sedimentation, fault-slip and subsidence rates. *Tectonophysics*, **440**, 29–51.

Mack, G.H., Seager, W.R., Leeder, M.R., Perez-Arlucea, M. & Salyards, S.L. (2006) Pliocene and Quaternary history of the Rio Grande, the axial river of the southern Rio Grande rift, New Mexico, USA. *Earth Sci. Rev.*, **79**, 141–162.

Malartre, F., Ford, M. & Williams, E.A. (2004) Preliminary biostratigraphy and 3D geometry of the Vouraikos Gilbert-type fan delta, Gulf of Corinth, Greece. *C.R. Geosci.*, **336**, 269–280.

McClusky, S., Balassanian, S., Barka, A., Demir, C., Ergintav, S., Georgiev, I., Gurkan, O., Hamburger, M., Hurst, K., Kahle, H., Kastens, K., Kekelidze, G., King, R., Kotzev, V., Lenk, O., Mahmoud, S., Mishin, A., Nadariya, M., Ouzounis, A., Paradissis, D., Peter, Y., Prilepin, M., Reilinger, R., Sanli, I., Seeger, H., Tealeb, A., Toksoz, M.N. & Veis, G. (2000) Global Positioning System constraints on plate kinematics and dynamics in the eastern Mediterranean and Caucasus. *J. Geophys. Res.-Solid Earth*, **105**, 5695–5719.

McMurray, L.S. & Gawthorpe, R.L. (2000) Along-strike variability of forced regressive deposits: late Quaternary, northern Peloponnesos, Greece. In: *Sedimentary Response to Forced Regressions* (Ed. by Hunt D., Gawthorpe R.L.) *Geol. Soc. of London, Spec. Publ.*, pp. 363–377.

McNeill, L.C., Cotterill, C.J., Henstock, T.J., Bull, J.M., Stefatos, A., Collier, R., Papatheoderou, G., Ferentinos, G. & Hicks, S.E. (2005) Active faulting within the offshore western Gulf of Corinth, Greece: implications for models of continental rift deformation. *Geology*, **33**, 241–244.

Moretti, I., Lykousis, V., Sakellariou, D., Reynaud, J.Y., Benziane, B. & Prinzhoffer, A. (2004) Sedimentation and subsidence rate in the Gulf of Corinth: what we learn from the Marion Dufresne's long-piston coring. *C.R. Geosci.*, **336**, 291–299.

Morewood, N.C. & Roberts, G.P. (2002) Surface observations of active normal fault propagation: implications for growth. *J. Geol. Soc.*, **159**, 263–272.

Nixon, C.W., McNeill, L.C., Bull, J.M., Bell, R.E., Gawthorpe, R.L., Henstock, T.J., Christodoulou, D., Ford, M., Taylor, B., Sakellariou, D., Ferentinos, G., Papatheodorou, G., Leeder, M.R., Collier, R.E.L., Goodliffe, A.M., Sachpazi, M. & Kranis, H. (2016) Rapid spatiotemporal variations in rift structure during development of the Corinth Rift, central Greece. *Tectonics*, **35**, 1225–1248.

Ori, G.G. (1989) Geologic history of the extensional basin of the Gulf of Corinth (Miocene-Pleistocene), Greece. *Geology*, **17**, 918–921.

Palyvos, N., Lemeille, F., Sorel, D., Pantosti, D. & Pavlopoulos, K. (2008) Geomorphic and biological indicators of paleoseismicity and Holocene uplift rate at a coastal normal fault footwall (western Corinth Gulf, Greece). *Geomorphology*, **96**, 16–38.

Palyvos, N., Mancini, M., Sorel, D., Lemeille, F., Pantosti, D., Julia, R., Triantaphyllou, M. & De Martini, P.M. (2010) Geomorphological, stratigraphic and geochronological evidence of fast Pleistocene coastal uplift in the westernmost part of the Corinth Gulf Rift (Greece). *Geol. J.*, **45**, 78–104.

Papatheodorou, G. & Ferentinos, G. (1993) Sedimentation processes and basin-filling depositional architecture in an active asymmetric graben: Strava graben, Gulf of Corinth, Greece. *Basin Res.*, **5**, 235–253.

Pedley, H.M. (1990) Classification and environmental models of cool freshwater tufas. *Sed. Geol.*, **68**, 143–154.

Pirazzoli, P.A., Stiros, S.C., Fontugne, M. & Arnold, M. (2004) Holocene and Quaternary uplift in the central part of the southern coast of the Corinth Gulf (Greece). *Mar. Geol.*, **212**, 35–44.

Portman, C., Andrews, J.E., Rowe, P.J., Leeder, M.R. & Hoogewerff, J. (2005) Submarine-spring controlled calcification and growth of large Rivularia bioherms, Late Pleistocene (MIS 5e), Gulf of Corinth, Greece. *Sedimentology*, **52**, 441–465.

Prosser, S. (1993) Rift-Related Linked Depositional Systems and Their Seismic Expression. In: *Tectonics and Seismic Sequence Stratigraphy* (Ed. Williams G.D. & Dobb A.) *Geol. Soc., London, Special Publ.*, **71**, 35–66.

Ravnas, R. & Steel, R.J. (1998) Architecture of marine rift-basin successions. *Bull. Am. Associat. Petrol. Geol.*, **82**, 110–146.

Roberts, G.P., Houghton, S.L., Underwood, C., Papanikolaou, I., Cowie, P.A., van Calsteren, P., Wigley, T., Cooper, F.J., McArthur, J.M. (2009) Localization of Quaternary slip rates in an active rift in 10(5) years: an example from central Greece constrained by U-234-Th-230 coral dates from uplifted paleoshorelines. *J. Geophys. Res. Solid Earth*, **114**, https://doi.org/10.1029/2008jb005818.

Rohais, S., Eschard, R., Ford, M., Guillocheau, F. & Moretti, I. (2007a) Stratigraphic architecture of the Plio-Pleistocene infill of the Corinth Rift: implications for its structural evolution. *Tectonophysics*, **440**, 5–28.

Rohais, S., Joannin, S., Colin, J.P., Suc, J.P., Guillocheau, F. & Eschard, R. (2007b) Age and environmental evolution of the syn-rift rill of the southern coast of the gulf of Corinth (Akrata-Derveni region, Greece). *Bull. Soc. Geol. Fr.*, **178**, 231–243.

Rohais, S., Eschard, R. & Guillocheau, F. (2008) Depositional model and stratigraphic architecture of rift climax Gilbert-type fan deltas (Gulf of Corinth, Greece). *Sed. Geol.*, **210**, 132–145.

Sakellariou, D., Lykousis, V., Alexandri, S., Kaberi, H., Rousakis, G., Nomikou, P., Georgiou, P. & Ballas, D. (2007) Faulting, seismic-stratigraphic architecture and Late Quaternary evolution of the Gulf of Alkyonides Basin-East Gulf of Corinth, Central Greece. *Basin Res.*, **19**, 273–295.

Seger, M. & Alexander, J. (1993) Distribution of Plio-Pleistocene and Modern coarse-grained deltas south of the Gulf of Corinth, Greece. In: *Tectonic Controls and Signatures in Sedimentary Successions* (Ed. by Frostick L.E. & Steel R.J.) *Int. Assoc. Sedimentol. Spec. Publ.*, **20**, 37–48.

Skourtsos, E. & Kranis, H. (2009) Structure and evolution of the western Corinth Rift, through new field data from the Northern Peloponnesus. In: *Extending a Continent: Architecture, Rheology and Heat Budget* (Ed. by Ring U. & Wernicke B.) Geological Society, London, Special Publications. **321**, 119–138.

Skourtsos, E., Kranis, H., Zambetakis-Lekkas, A., Gawthorpe, R.L. & Leeder, M.R. (2016) Alpine basement outcrops at northern Peloponnesus: implications for the early stages in the evolution of the Corinth Rift. *Bull. Geol. Soc. Greece*, **50**, 153–163.

Taylor, B., Weiss, J.R., Goodliffe, A.M., Sachpazi, M., Laigle, M. & Hirn, A. (2011) The structures, stratigraphy and evolution of the Gulf of Corinth rift, Greece. *Geophys. J. Int.*, **185**, 1189–1219.

Turner, J.A., Leeder, M.R., Andrews, J.E., Rowe, P.J., van Calsteren, P. & Thomas, L. (2010) Testing rival tectonic uplift models for the Lechaion Gulf in the Gulf of Corinth rift. *J. Geol. Soc.*, **167**, 1237–1249.

Zelilidis, A. (2000) Drainage evolution in a rifted basin, Corinth graben, Greece. *Geomorphology*, **35**, 69–85.

Manuscript received 10 March 2017; In revised form 20 July 2017; Manuscript accepted 1 August 2017.